Article

Cell Reports

Concomitant Infection of *S. mansoni* and *H. pylori* Promotes Promiscuity of Antigen-Experienced Cells and Primes the Liver for a Lower Fibrotic Response

Graphical Abstract

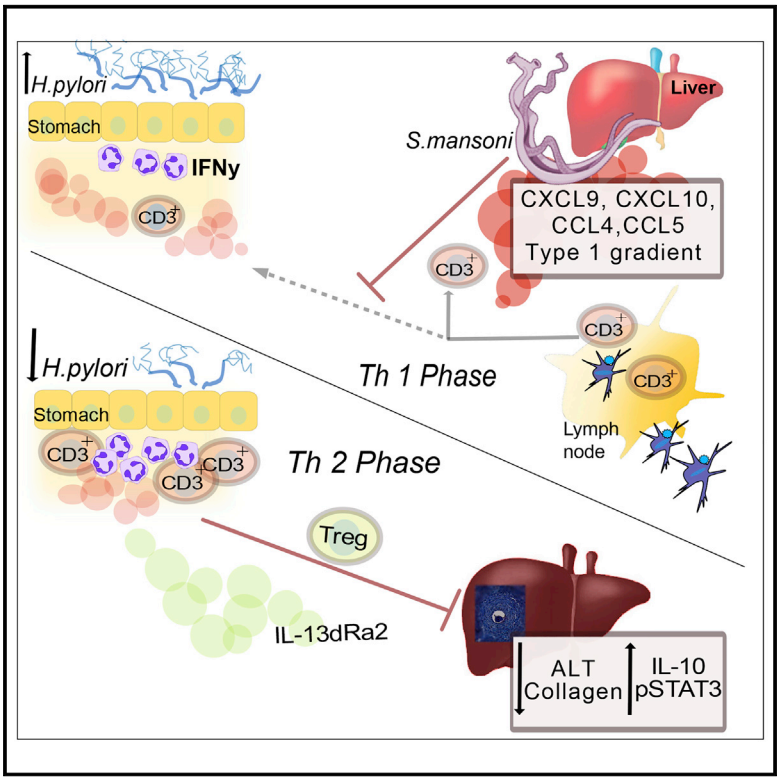

Authors

Sonakshi Bhattacharjee, Raquel Mejías-Luque, Eva Loffredo-Verde, Albulena Toska, Michael Flossdorf, Markus Gerhard, Clarissa Prazeres da Costa

Correspondence

markus.gerhard@tum.de (M.G.), clarissa.dacosta@tum.de (C.P.d.C.)

In Brief

Co-infection is ubiquitous in human populations and is yet not the most widely studied experimental topic. Bhattacharjee et al. demonstrate that the immunological interaction of two prominent, anatomically isolated human pathogens, *H. pylori* and *S. mansoni*, eventually results in an unusual, mutually ameliorating effect on the detrimental course of both infections.

Highlights

- Co-infection of *H. pylori* and *S. mansoni* results in altered disease-specific pathology
- *S. mansoni* infection induces misdirection of *H. pylori*-associated CXCR3^{+} T cells
- Immune misdirection of cells is helminth-immune-phase dependent
- *H. pylori* infection ameliorates schistosome-associated liver fibrosis

Bhattacharjee et al., 2019, Cell Reports *28*, 231–244
July 2, 2019
https://doi.org/10.1016/j.celrep.2019.05.108

CellPress

Cell Reports
Article

Concomitant Infection of *S. mansoni* and *H. pylori* Promotes Promiscuity of Antigen-Experienced Cells and Primes the Liver for a Lower Fibrotic Response

Sonakshi Bhattacharjee,[1,3] Raquel Mejías-Luque,[1,3] Eva Loffredo-Verde,[2] Albulena Toska,[1] Michael Flossdorf,[1] Markus Gerhard,[1,3,4,*] and Clarissa Prazeres da Costa[1,4,5,*]
[1]Institute for Medical Microbiology, Immunology and Hygiene, Technical University of Munich, Munich, Germany
[2]Institute for Virology, Technical University of Munich, Munich, Germany
[3]German Centre for Infection Research (DZIF), partner site Munich, Munich, Germany
[4]These authors contributed equally
[5]Lead Contact
*Correspondence: markus.gerhard@tum.de (M.G.), clarissa.dacosta@tum.de (C.P.d.C.)
https://doi.org/10.1016/j.celrep.2019.05.108

SUMMARY

Helicobacter pylori chronically colonizes the stomach and is strongly associated with gastric cancer. Its concomitant occurrence with helminths such as schistosomes has been linked to reduced cancer incidence, presumably due to suppression of *H. pylori*-associated pro-inflammatory responses. However, experimental evidence in support of such a causal link or the mutual interaction of both pathogens is lacking. We investigated the effects of co-infection during the different immune phases of *S. mansoni* infection. Surprisingly, co-infected mice had increased *H. pylori* gastric colonization during the interferon gamma (IFNγ) phase of schistosome infection but reduced infiltration of T cells in the stomach due to misdirection of antigen-experienced CXCR3$^+$ T cells to the liver. Unexpectedly, *H. pylori* co-infection resulted in partial protection from schistosome-induced liver damage. Here, we demonstrate that an increase in fibrosis-protective IL-13Ra2 is associated with *H. pylori* infection. Thus, our study strongly points to an immunological interaction of anatomically isolated pathogens, eventually resulting in altered disease pathology.

INTRODUCTION

Helicobacter pylori colonizes the stomachs of about 4.4 billion people with a significant percentage developing gastric tumors, the fourth most common cause of cancer-related death worldwide (Hooi et al., 2017; World Health Organization, 2017). Accumulating evidence suggests that the inflammatory processes leading to gastric cancer are influenced by a variety of factors including genetic predisposition, diet, *H. pylori* strain type, and interestingly co-infections with helminths (Shimizu et al., 2017; Balakrishnan et al., 2017; Ogawa et al., 2017).

Since *H. pylori* induces a strong T helper Th1/Th17 driven inflammatory response, helminths like *Schistosoma mansoni* that drive a chronic type 2/Treg response have been suggested to skew this classical inflammatory response (Abou Holw et al., 2008; Du et al., 2006). However, *S. mansoni* infection gives rise to different immune phases during its distinct developmental stages within the human host. The initial infection occurs when cercariae, derived from freshwater snails, penetrate skin and enter the circulation. The acute Th1 phase is associated with increased interferon gamma (IFNγ) levels and is caused due to the early, mainly migrating and maturing stages of *S. mansoni* close to the portal vein. This is replaced by strong type 2 immune responses after 8–9 weeks when adult worms reside in the mesenteric vasculature and the fecund females begin to release eggs (Teixeira-Carvalho et al., 2008). This phase is eventually superseded by a strong immune-regulatory response with components like Treg and Breg that constitute the complex type 2 or chronic phase (Layland et al., 2010; Haeberlein et al., 2017; McKee and Pearce, 2004). These dynamic immune profiles could have very different effects on *H. pylori* infection and gastric inflammation.

On the other hand, schistosomiasis is in itself a debilitating disease causing 200,000 deaths per year as well as 3.3 million disability adjusted life years (DALYs) mainly associated with liver fibrosis and portal hypertension (Global Atlas of Helminth Infection, 2010). The main pathology caused by the hepato-intestinal form of schistosomiasis is due to granuloma formation around eggs trapped primarily in the liver (Ali et al., 2017; Burke et al., 2009). The fibrotic processes are multifaceted and involve several cell types. Th2 cells and innate lymphoid cells 2 (ILC2) induced by decaying eggs contribute to the release of IL-13, which binds to its classical receptor on fibroblasts and macrophages (Gieseck et al., 2016; Fairfax et al., 2012). Stimulated fibroblasts differentiate into myofibroblasts and produce extracellular matrix (ECM). IL-13 also induces several genes including interstitial collagens, tissue inhibitors of matrix metalloproteinases (TIMP), fibrillin, and tenascin, all involved in the development of fibrosis. As collagen replaces the hepatocytes around the egg, there is a slow progression to a fibrotic liver (Gieseck et al., 2016; Wynn, 2003). This pathway is regulated by polarized Th1 cells that compete with Th2 cells for arginine as well as CD4$^+$

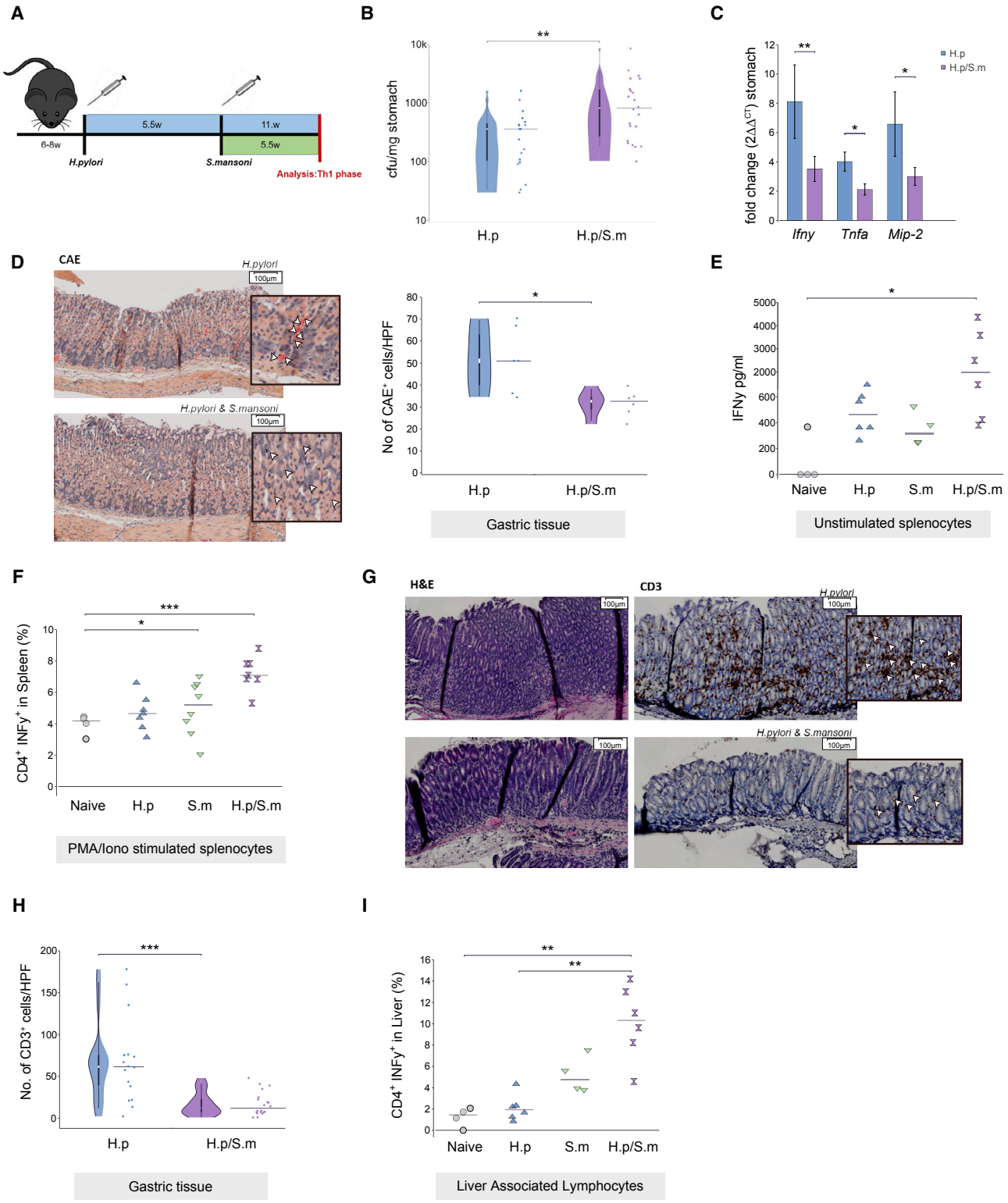

Figure 1. Higher *H. pylori* Colonization and Lower Inflammation during the Th1 Phase of *S. mansoni* Infection

(A) *In vivo* infection model for the acute/Th1 phase.

(B) Elevated colony forming units (CFUs) from stomach isolate in concurrently infected mice at 5.5 weeks post helminth infection.

(C) mRNA fold change (over naive mice) of *Ifn-γ*, *Tnf-α*, and *Mip-2* in the stomach during the Th1 phase.

(legend continued on next page)

regulatory T cells and B cells that produce IL-10 (Layland et al., 2007; Sadler et al., 2003; Erhardt et al., 2007). Most importantly though, the IL-13 decoy Ra2 (IL-13dRa2) is the strongest modulator of this pathway, especially in schistosomiasis (Mentink-Kane et al., 2004; Gatlin et al., 2009; Chiaramonte et al., 1999). This scavenger receptor is induced in parallel with IL-13 and is an important factor for determining the amount of free IL-13. IL-13dRa2 has thus been shown to not only be host protective but also prolong host survival during schistosomiasis (Chiaramonte et al., 1999; Mentink-Kane et al., 2004). Significant efforts have focused on attempts to understand the regulation of this fibrotic disease, with studies analyzing the effects of immune strategies on pathways associated with collagen deposition in the liver. Quite recent evidence has suggested that *H. pylori* may be associated with a variety of extra-gastric diseases as well, including liver and pancreatic disease (Franceschi et al., 2014; Rabelo-Gonçalves et al., 2015). Infection with the bacterium has been correlated with progression of non-alcoholic fatty liver disease, hepatitis C infection, and hepatocellular carcinoma (HCC), further underlining its possible systemic immunomodulatory capacities on other inflammatory processes (Rocha et al., 2005; Xuan et al., 2006).

Even though schistosomiasis is endemic in 78 countries (World Health Organization, 2019) with a high prevalence of *H. pylori* infection, the interaction of both pathogens has not been studied in any experimental model up until now.

Employing an experimental co-infection model, we demonstrate the impact of co-infection on disease parameters affecting both pathogens. While our data suggest that acute concomitant *S. mansoni* infection results in the reduction of *H. pylori*-driven gastric inflammation as shown for some other helminths, it is not due to the helminth-driven type 2 response (Fox et al., 2000). Unexpectedly, we observed this protection during the Th1 phase of helminth infection, which we show here to be driven by misdirection of T cells. Intriguingly, we also observed a positive effect of *H. pylori* infection on *S. mansoni*-associated liver disease in terms of reduced hepatic cell damage and fibrosis. Our study points to an unusual, mutual ameliorating effect of the two pathogens on the detrimental course of both chronic infections.

RESULTS

Concomitant Acute Schistosomiasis Increases *H. pylori* Colonization and Reduces Inflammation in the Stomachs of Co-infected Mice

To mimic the most likely infection scenario in humans where *H. pylori* infection precedes schistosome infection due to *H. pylori* transmission within the family or from the mother to child (Allaker et al., 2002; Cervantes et al., 2010; Miyaji et al., 2000; Rothenbacher et al., 2000; Spencer et al., 2017; Alemayehu and Tomass, 2015), we first infected C57BL/6 mice with *H. pylori* (PMSS1). 5.5 weeks later, when *H. pylori* infection reaches chronicity, these mice were subcutaneously infected with *S. mansoni*. After 5.5 weeks of schistosome infection (corresponding to the peak of the Th1 phase) (Figures 1A and S1A), we investigated *H. pylori* colonization and gastric inflammation.

Since *H. pylori* colonization is known to be controlled throughout the course of infection by Th1/Th17 responses, with IFNγ as a major mediator of bacterial clearance, we were surprised to find significantly increased *H. pylori* colonization in the stomach during this Th1-prone phase of helminth infection (Figure 1B). This was accompanied by reduced mRNA expression levels of *Ifnγ*, *Tnf-α*, and *Mip-2* (IL-8 homolog) and lower pathological scores in gastric tissue of co-infected mice compared to *H. pylori* mono-infected (H.p) mice (Figures 1C and S1B). Lower *Mip-2* levels additionally correlated with reduced neutrophil counts in the stomachs of co-infected animals (Figure 1D). Of note, as comparable to naive animals, *S. mansoni* mono-infected (S.m) mice had no inflammation in gastric tissue (Figures S1B and S1C). In order to determine if co-infection with *S. mansoni* altered *H. pylori*-associated T cell responses systemically in terms of number or functionality, we measured IFNγ production from unstimulated splenocytes as well as proportions of $CD4^+$/$CD8^+$ $IFN\gamma^+$ cells after stimulation (Figures 1E, 1F, S1D, and S1E). Interestingly, we observed higher levels of IFNγ production from lymphocytes of co-infected mice compared to the mono-infected groups, indicating that T cell activation was not universally inhibited, but those circulating effector T cell populations may have failed to migrate to the gastric mucosa. Indeed, correlating with increased *H. pylori* colonization, the infiltration of $CD3^+$ cells was significantly lower in gastric tissue from co-infected mice (Figures 1G and 1H). These findings indicate that schistosome-induced systemic IFNγ, e.g., as measured in the spleen, may not contribute locally to control *H. pylori* growth in the stomach. Rather, the infiltration of inflammatory T cells to the stomach was hindered during co-infection.

Misdirection of Antigen-Experienced Cells during Co-infection Results in Reduced Gastric Inflammation

We hypothesized that during co-infection, *H. pylori*-associated effector T cells may be misdirected to a different anatomical site, such as the liver, where acute *S. mansoni* infection initiates

(D) Quantification of chloracetate esterase positive (CAE^+) cells (neutrophils) from gastric samples during the Th1 phase of helminth infection and representative stainings (average of 5 fields with 40x magnification). Arrows point to cell infiltration.
(E) Increased IFNγ production in unstimulated splenocytes of co-infected mice after 48 h in culture.
(F) Increased frequencies of IFNγ-producing $CD4^+$ effector cells in co-infected mice compared to H.p mice, gated on all living lymphocytes, within spleen, stimulated with phorbol myristate acetate (PMA)/ionomycin.
(G) Immunohistochemistry staining of CD3+ infiltration from gastric samples during the Th1 phase of helminth infection.
(H) Quantification of $CD3^+$ infiltration from gastric samples during the Th1 phase of helminth infection (average of 5 fields with 40x magnification). Arrows point to immune cell infiltration.
(I) Increased frequencies of IFNγ-producing $CD4^+$ effector cells in co-infected mice compared to H.p mice, gated on all living lymphocytes, within liver, stimulated with PMA and ionomycin.
Data are shown as group median, 3 independent experiments with at least n = 3 per group. *$p < 0.05$, **$p < 0.01$, and ***$p < 0.001$.

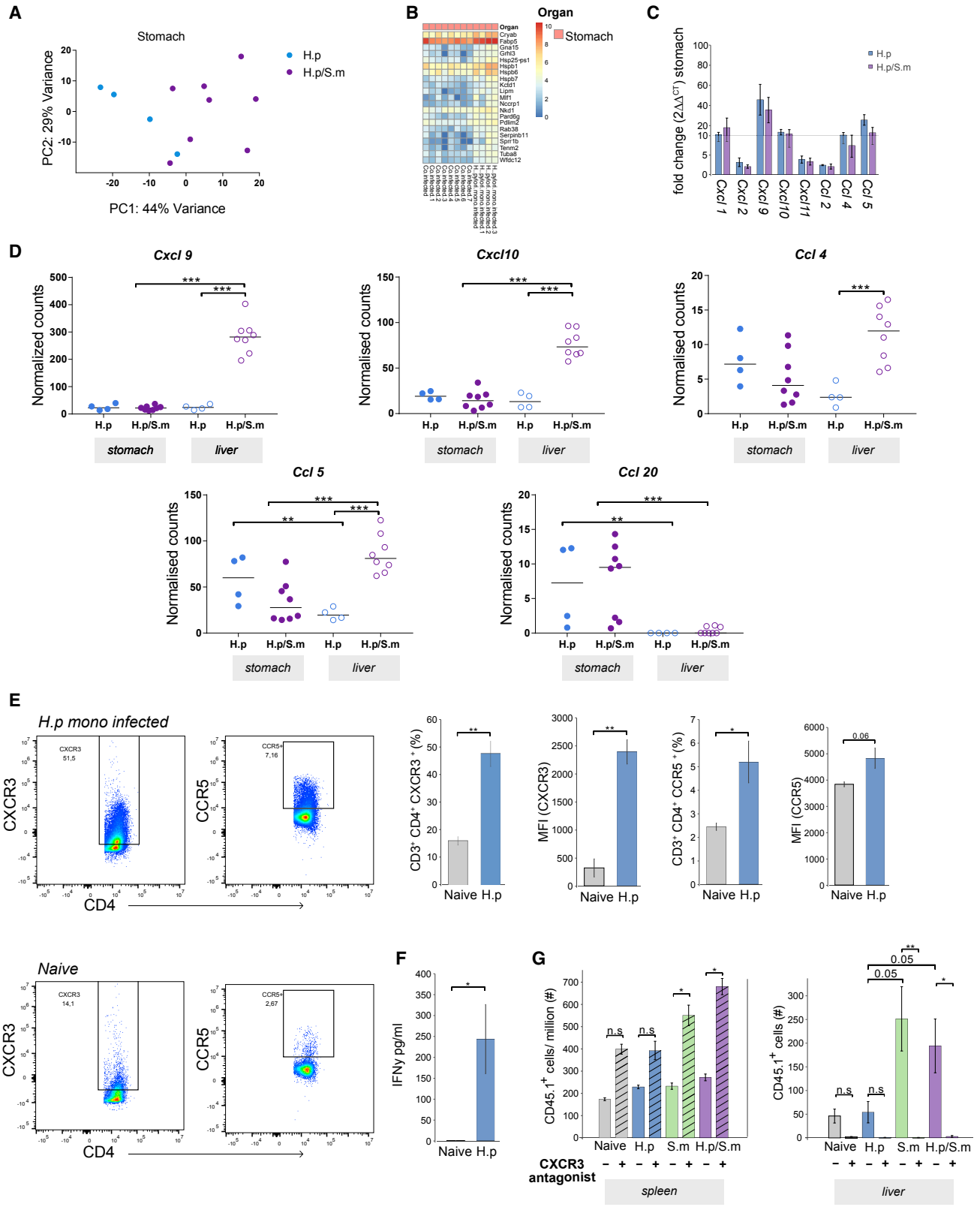

(legend on next page)

a potent chemokine-driven inflammatory response, which is a phenomenon independent of effective antigen priming, specificity, and T cell functionality. Indeed, we detected higher frequencies of IFNγ producing $CD4^+$ T cells in liver-associated lymphocytes (LALs) from co-infected mice (Figure 1I). However, this process would require a stronger gradient of type 1 chemokines (associated with the respective type 1 receptors CXCR3 and CCR5) in the liver compared to the stomach. RNA sequencing (RNA-seq) of the stomachs revealed major differences in RNA expression between *H. pylori* mono- and co-infected mice (Figure 2A), but the majority of the differentially expressed genes were not associated with chemokines (Figure 2B). Contrary to decreased *Ifnγ*, *Tnf-α,* and *Mip-2* (*cf.* Figure 1C), other chemokines associated with homing of type 1 cells (*Cxcl9, Cxcl10, Cxcl11, Ccl5*) that were upregulated during *H. pylori* infection in the stomach remained similarly induced during both mono- and co-infection (Figure 2C). However, upon comparing gene expression in the stomach and the liver, a number of pro-inflammatory chemokines (*Cxcl9*, *Cxcl10*, *Ccl4*, *Ccl5*) were significantly upregulated in the livers of co-infected compared to H.p mice (Figure 2D). Interestingly, however, *Ccl20* was not upregulated in the livers of co-infected mice (Figure 2D); this chemokine has been shown to attract regulatory T cells into the stomach during *H. pylori* infection (Cook et al., 2014). This indicates a predilection and selectivity toward increased type 1 chemokines, thus primarily affecting the homing of only type 1 cells with corresponding receptors into gastric tissue.

In order to further investigate if T cells with an antigen-experienced phenotype were being misdirected to the liver in the Th1 phase, we performed adoptive transfers of $CD4/CD8^+$ $CD44^{hi}$ T cells isolated only from *H. pylori*-priming-associated organs (stomach, mesenteric lymph nodes [MLNs], and Peyer's patches). Acquired cells from *H. pylori*-infected animals expressed high levels of type 1 chemokine receptors CXCR3 and to a lower extent CCR5, compared to those harvested from naive mice (Figure 2E). Additionally, when re-stimulated with *H. pylori* lysate overnight, they produced significantly higher IFNγ (Figure 2F). These cells, derived from *H. pylori*-infected (5.5 weeks) $CD45.1^{+/+}$ mice were adoptively transferred into wild-type (WT) ($CD45.2^{+/+}$) mice in four different experimental groups: naive, H.p, S.m, and co-infected (H.p/S.m) (Figures S2A, S2B, and S2C). After 3 days, proportions of donor $CD45.1^+$ cells were analyzed in the stomach, liver, lung, spleen, MLNs, and blood of all animals. While the lymphoid organs (spleen and MLN), stomach, and lungs did not show differences between the groups (Figures 2G and S2D), the co-infected mice had higher frequencies and absolute numbers of $CD45.1^+$ cells in the livers when compared to naive and H.p mono-infected mice (Figures 2G and S2E). To conclusively determine if high expression of CXCR3 was required to misdirect cells into the liver, we blocked the receptor on $CD45.1^{+/+}$ cells before transfer using an allosteric inhibitor of CXCR3. Interestingly, these cells increased in circulation (within the spleen) and infiltration of CXCR3-ablated cells was dramatically reduced in *S. mansoni*-infected livers (Figure 2G). As observed in the original experiment, the adoptively transferred animals still displayed a similar phenotype of increased colonization in the gastric tissue (Figure S2F). Additionally, parameters affecting *S. mansoni* type 1 responses remained unchanged (Figure S2G). Interestingly, we observed recruitment of a proportion of T cells in naive and *S. mansoni* stomachs (Figure S2D). A probable explanation is that these cells were initially isolated from the stomach of *H. pylori*-infected mice before transfer and thus bear integrin receptors particular to this organ. Therefore, these cells are found circulating in the stomachs of all groups.

H. pylori Colonization and Gastric Inflammation Stabilize during the Th2/Chronic Phase of Helminth Infection

S. mansoni elicits dynamic, successive, and distinct immune responses depending on its developmental stage in the host. Since we hypothesized that these individual phases will have very distinct effects on the outcome of *H. pylori* co-infection, we next analyzed the outcome of *H. pylori*-induced immune responses during the peak of the Th2 phase of the helminth infection. Again, mice were infected with *H. pylori* for 5.5 weeks before the infection with schistosomes, then sacrificed during the peak of the Th2 phase after 9.5 weeks of helminth infection (Figure 3A). In contrast to the Th1 phase, bacterial load in the stomachs of both H.p and co-infected mice were similar during the Th2 phase of *S. mansoni* infection (Figure 3B). Additionally, we observed that the inflammatory parameters in co-infected mice matched those of their H.p counterparts (Figures 3C and S3A). The systemic IFNγ levels in the spleen were also similar between co-infected and mono-infected groups (Figure 3D). In accordance with the colonization, infiltration of $CD3^+$ cells into stomach tissue of co-infected mice was now comparable to the H.p group (Figures 3E and 3F). Proportions of $CD4^+IFN\gamma^+$ cells in the liver were now similar between both *S. mansoni*-infected groups as well (Figure 3G). Finally, as

Figure 2. Higher Expression of Type 1 Chemokines in Livers of Co-infected Mice Leads to Immune Misdirection of $CXCR3^+$ T Cells

(A) Principal component (PC) analysis of the stomach between co-infected and H.p mice.

(B) Heatmap of differentially expressed genes in the stomach between co-infected and H.p mice.

(C) mRNA fold change (over naive mice) of type 1 chemokines in the stomach during the Th1 phase of helminth infection.

(D) Expression of *Cxcl9*, *Cxcl10*, *Ccl4*, *Ccl5*, and *Ccl20* in the stomach and liver of co-infected and H.p animals as analyzed by RNA-seq during the Th1 phase (filled dots representing stomach, open dots representing liver). Read counts are normalized with respect to differences in library size.

(E) Type 1 chemokine receptor expression (CXCR3 and CCR5) on cells harvested from stomach, Peyer's patches, and mesenteric lymph nodes of *H. pylori*-infected and naive mice (frequency and mean fluorescence intensity [MFI]).

(F) IFNγ secreted by cells acquired from stomach, Peyer's patches, and mesenteric lymph nodes of *H. pylori*-infected and naive mice, re-stimulated with *H. pylori* lysate overnight.

(G) 100,000 CD45.1 $CD4/CD8$ $CD44^{hi}$ cells isolated from *H. pylori*-infected mice (treated with CXCR3 inhibitor or left untreated) were adoptively transferred into wild-type infected or uninfected animals. 3 days post transfer, cells were analyzed through flow cytometry.

Adjusted for multiple testing: *$p < 0.05$, **$p < 0.01$, and ***$p < 0.001$. Data are shown as group median or mean ± SEM for (C), (E), (F), and (G); 2 independent experiments with at least n = 3 per group.

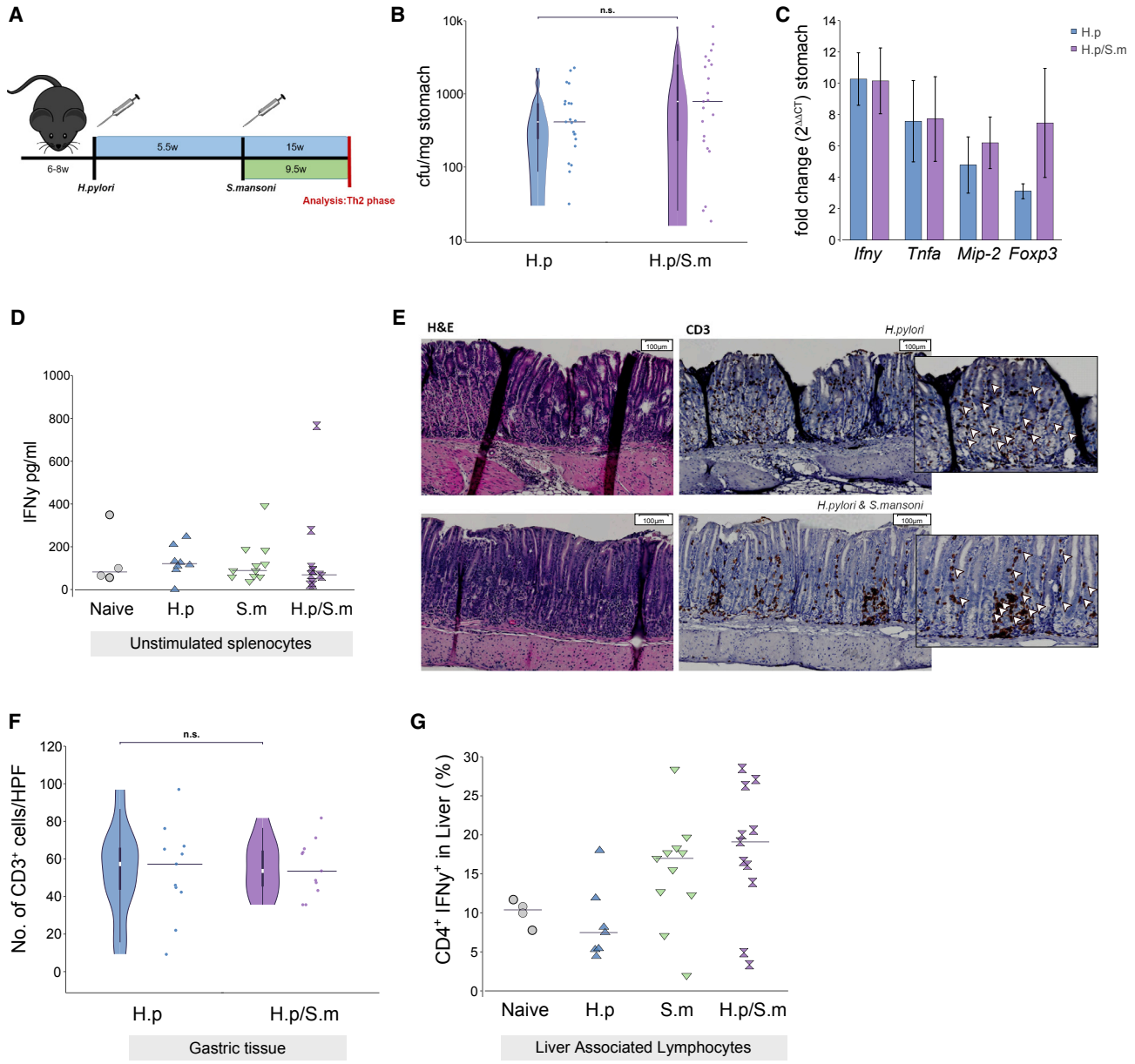

Figure 3. *H. pylori* Colonization and Gastric Inflammation Stabilize during the Th2/Chronic Phase of Helminth Infection

(A) *In vivo* infection model for the chronic/Th2 phase.

(B) Colony forming units (CFUs) from stomach isolate in concurrently infected mice compared to H.p mice at 9.5 weeks post helminth infection.

(C) mRNA fold change (over naive mice) of *Ifn-*γ, *Tnf-*α, *Mip-2*, and *Foxp3* in the stomach during the Th2 phase.

(D) IFNγ production in unstimulated splenocytes of co-infected mice after 48 h in culture.

(E) Immunohistochemistry staining of $CD3^+$ infiltration from gastric samples during the Th1 phase of helminth infection.

(F) Quantification of $CD3^+$ infiltration from gastric samples during the Th2 phase of helminth infection (average of 5 fields with 40x magnification). Arrows point to immune cell infiltration.

(G) Frequencies of IFNγ-producing $CD4^+$ effector cells in co-infected mice compared to H.p mice, gated on all living lymphocytes, within liver, stimulated with PMA and ionomycin.

Data are shown as group median, 3 independent experiments with at least n = 3 per group. *p < 0.05, **p < 0.01, and ***p < 0.001.

determined by RNA-seq, the expression of *Cxcl9*, *Cxcl10*, and *Ccl5* in livers of co-infected mice were much lower in the Th2 phase compared to the Th1 phase, with many type 1 chemokines being no longer detectable (Figure S3B). These results indicate that helminth-induced type2 responses lead to altered cytokine and especially chemokine milieu within the liver; the initial type 1 chemokine gradient subsides and thus allows appropriate homing of the *H. pylori*-induced T cells.

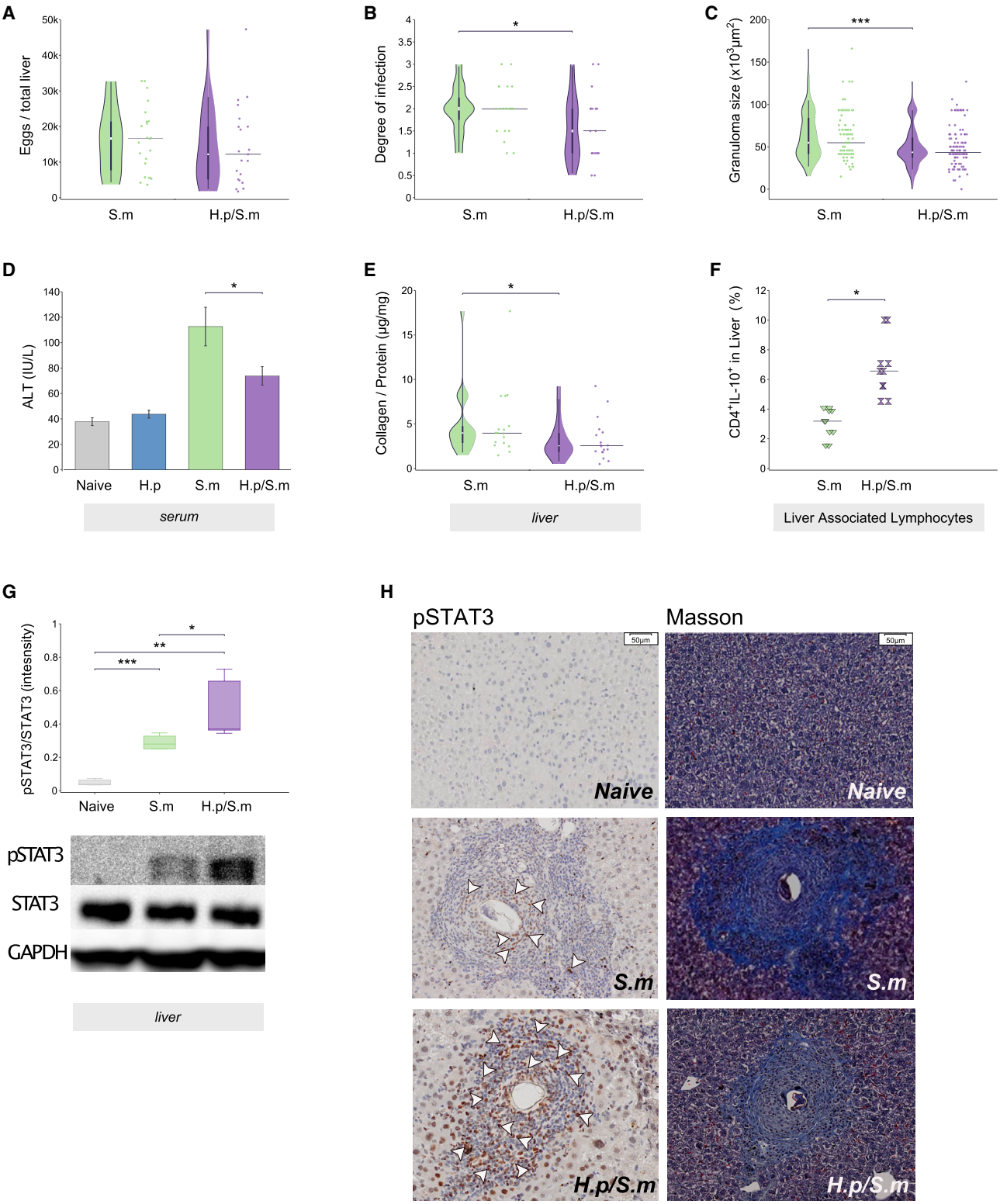

Figure 4. Co-infected Mice Have Lesser Liver Pathology and Damage in the Th2 Phase

(A) Egg count within liver samples between both groups.

(B) Visual estimation of the granulomas observed in fresh liver samples display lower degree of infection for co-infected mice compared to S.m mice. Qualitative grades (1+, 2+, 3+) are based on progression of fibrosis based on stiffness, color, and gross morphology of the liver.

(legend continued on next page)

Taken together, concurrent infection of *S. mansoni* with *H. pylori* induces misdirection of CXCR3$^+$ antigen-experienced T cells to the liver instead of gastric tissue where, as a consequence, reduced effector responses in the Th1 phase result in increased *H. pylori* colonization.

Concomitant *H. pylori* Reduces Liver Pathology Elicited by *S. mansoni* Infection

Next, we investigated how *H. pylori* co-infection influenced *S. mansoni* infection parameters and the ensuing immunopathology during both the Th1 and Th2 phases of helminth infection. Concerning antigen-specific immune responses after stimulation with soluble egg antigens (SEAs), we did not observe any differences in IFNγ, IL-10, or IL-13 secretion from splenocytes in either the Th1 or Th2 phase (Figures S4A and S4B). Additionally, we could not detect differences in the worm burden or egg numbers between the livers of mono- and co-infected mice (Figures 4A and S4C). The most striking pathological observation, however, was that the degree of infection (visual grading of egg-induced liver damage) was significantly reduced (Figures 4B and S4D). This was accompanied by substantially smaller liver granulomas (Figures 4C and S4E). Consequently, alanine aminotransferase (ALT) levels (a measure of liver cell destruction or disease) in the serum as well as collagen levels in the liver were significantly reduced in the co-infected group (Figures 4D and 4E).

We and others have shown previously that granuloma size as well as the extent of Th2 immune responses and thus fibrosis is strongly controlled by IL-10 and Treg, which are detected mainly in the circumference of the granulomas (Layland et al., 2007, 2010). Interestingly, while frequencies of Foxp3$^+$ cells in the liver were hardly affected in co-infected mice, they were accompanied by a significantly higher propensity of CD4$^+$ LALs to produce IL-10 (Figures 4F, S4F, and S4G). IL-10 is the most important regulatory cytokine during the Th2 phase of hepatic schistosomiasis, and the receptor for this molecule exists on almost every cell type involved during granuloma formation including hepatocytes and Kupffer cells (Mathurin et al., 2002; Knolle et al., 1998; Wang et al., 2011a). Therefore, we determined the localization and protein levels of IL-10 in the livers of co-infected and S.m animals. We observed increased IL-10 levels in liver lysates of co-infected mice (Figure S4H), predominantly localized in the periphery of granulomas (Figure S4I). We further examined if active IL-10 signaling through the fibrosis protective-STAT3 pathway was present in livers from co-infected animals. Remarkably, co-infected mice had higher pSTAT3 signaling in their livers compared to mono-infected mice (Figures 4G and 4H).

We next investigated how CD4$^+$ T cells could be polarized toward an IL-10-producing phenotype during co-infection. As both pathogens have been shown to target dendritic cells (DCs) to induce more tolerogenic T cells (Guiney et al., 2003; Kaebisch et al., 2014, 2016; Angeli et al., 2001; Jankovic et al., 2004; Everts et al., 2009), we looked more closely at the ability of antigen-presenting cells (APCs) to induce regulatory responses when exposed to both antigens. To investigate this, we performed co-culture *in vitro* assays using bone-marrow-derived dendritic cells (BMDCs). Upon stimulation with antigen mixtures from both pathogens together (SEA/*H. pylori*), BMDCs produced lower tumor necrosis factor alpha (TNF-α), similar levels of IL-12, but higher levels of IL-10 and IL-6 (Figures 5A and S5A) when compared to stimulation with individual antigens. Additionally, BMDCs exposed to both antigens showed decreased CD80/CD86 expression (similar to those exposed only to *H. pylori*) compared to BMDCs exposed to SEA alone (Figure S5B). When these primed BMDCs were co-cultured with CD4$^+$ cells from co-infected mice, we observed a significantly higher frequency of Foxp3$^+$ cells and a tendency for enhanced IL-10 production (Figure 5B), mimicking the results obtained during *in vivo* co-infection.

Apart from regulatory T cells, the extent of fibrosis is further kept in check by various factors regulating the IL-13 pathway including the IL-13dRa2 and IFNγ (Jimenez et al., 1984; Duncan and Berman, 1985; Layland et al., 2007). The former scavenges IL-13 and thus prevents binding of this pro-fibrotic cytokine to its own receptor and cells that produce the latter compete with the resources of Th2-producing cells, especially for arginine (Chiaramonte et al., 2003; Duncan and Berman, 1985; Jimenez et al., 1984). While there was a tendency for increased serum IL-13 (bound to IL-13dRa2) levels in co-infected mice during the Th1 phase, similar levels were observed between both *S. mansoni*-infected groups in the Th2 phase (Figure S5C). In line with this result, we detected significantly higher transcripts of *Il-13dRa2* in the livers of co-infected mice compared to mono-infected mice already in the Th1 phase of helminth infection, and this tendency was maintained well into the Th2 phase where overall expression of the *Il-13dRa* increased in both groups (Figure 5C). This pattern was reflected in the soluble levels of IL-13 dRa2 in the serum (Figure 5D). Interestingly, we observed no differences between markers of alternatively activated macrophages apart from a slight decrease in *Arginase 1* (*Arg1*) (Figure S5D).

In order to determine possible factors contributed by *H. pylori* infection that may mediate protection, we investigated the same pattern of transcripts in mono-infected mice. In both stomachs and livers of H.p mice, we detected higher levels of *IL-13dRa2*, *IL-10*, and *IFNγ* (Figure 5E). We could additionally detect increased levels of soluble IL-13dRα2 in the serum of these

(C) Granuloma size measured in liver sections by two independent observers.
(D) Serum alanine aminotransferase (ALT) levels as a measure of liver function.
(E) Collagen/mg protein levels measured in hydrolyzed liver tissue from *S. mansoni*-infected and co-infected mice.
(F) Increased frequencies of IL-10-producing CD4$^+$ effector cells in co-infected mice compared to S.m mice, gated on all living lymphocytes, within liver, stimulated with PMA and ionomycin.
(G) Western blot (densitometry quantification and membrane image) of pSTAT3 in whole liver lysates.
(H) Localization of pSTAT3 positive cells around eggs within granulomas in the liver, as observed by immunohistochemistry.
Data are shown as group median or mean ± SEM for (D) and (G), 3 independent experiments with at least n = 3 per group. *p < 0.05, **p < 0.01, and ***p < 0.001. Scale bars, 50 μm.

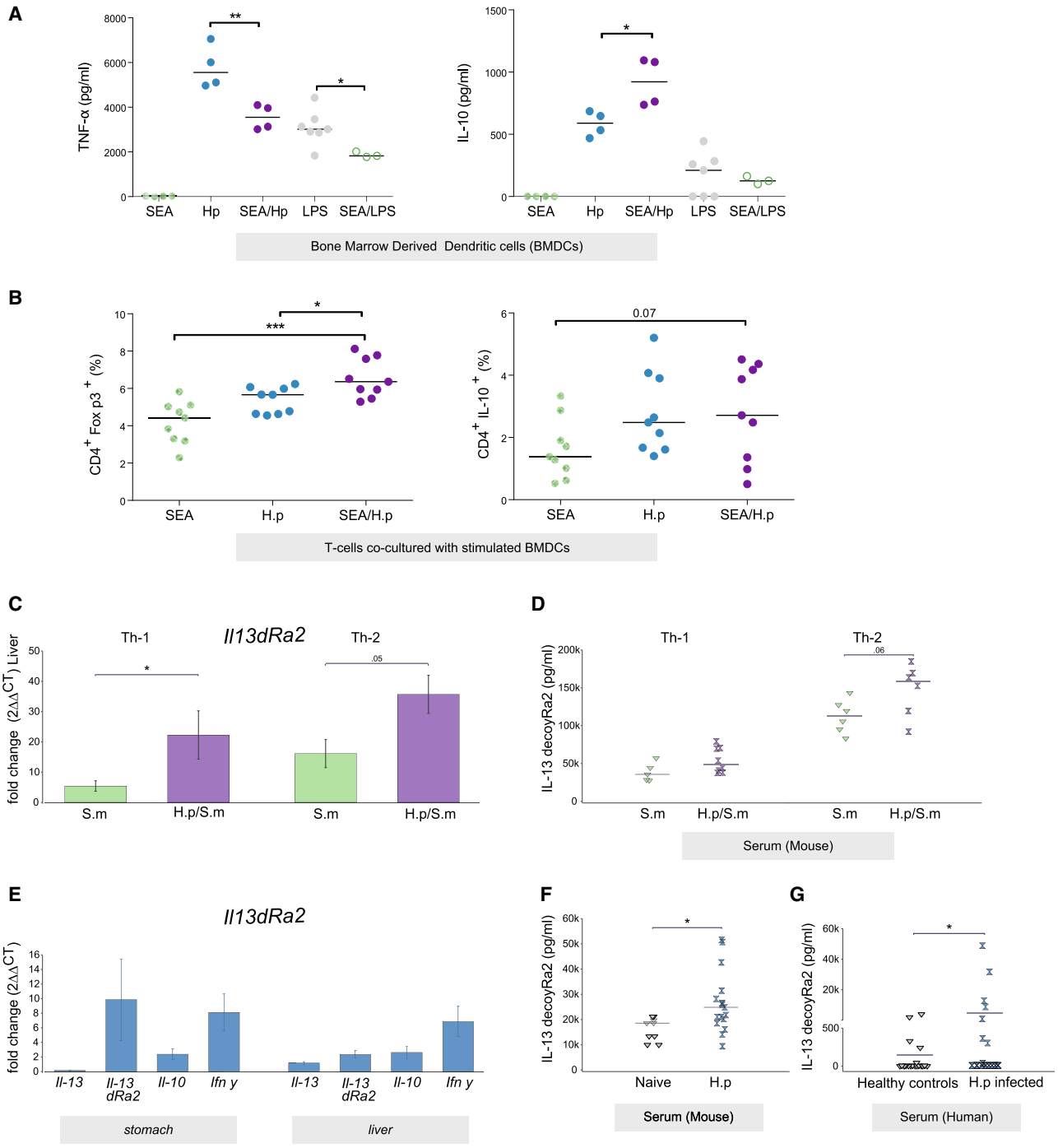

Figure 5. Co-infected Mice Have a Higher Propensity for Liver Protective Responses

(A) TNF-α and IL-10 levels in supernatants from BMDCs stimulated with either SEA (25 μg/ml), *H. pylori* PMSS1 live bacteria (MOI 5) or both, SEA (25 μg/ml), and live *H. pylori* bacteria (MOI 5).

(B) $CD4^+$ T cells from co-infected mice, co-cultured with stimulated BMDCs (see A) in a 2:1 ratio.

(C) mRNA fold change to naive mice of *Il-13decoy Ra2* in *S. mansoni* and co-infected mice during the Th1 and Th2 phases.

(D) Soluble levels of IL-13decoy Ra2 in serum of *S. mansoni* and co-infected mice during the Th1 and Th2 phases.

(E) mRNA fold change (over naive mice) of *IL-13*, *Il-13decoy ra2*, *Il-10*, and *Ifn-γ* in the stomach and liver of H.p mice measured by RT-PCR.

(F) Soluble levels of IL-13decoy Ra2 in serum of mice.

(G) Soluble levels of IL-13decoy Ra2 in serum of *H. pylori*-infected individuals compared to healthy non-infected controls.

Data are shown as group median, 3 independent experiments with at least n = 3 per group. *p < 0.05, **p < 0.01, and ***p < 0.001.

mice compared to naive animals (Figure 5F). Remarkably, this pattern was reflected in serum samples obtained from human *H. pylori*-infected individuals compared to healthy non-infected controls (Figure 5G).

These results collectively indicate that the consequence of *H. pylori* infection is not only localized to the stomach but may have potential effects in other organs such as the liver. Furthermore, we show an increase in IL-13dRa2 associated with *H. pylori* infection in both mouse and human. Together, we observe a partial protection in co-infected mice that we attribute to positive regulation of the IL-13 pathway by both pathogens, eventually reducing fibrosis and thus liver damage.

DISCUSSION

Co-infection is one of the most ubiquitous phenomena occurring in human populations and is yet not the most widely studied experimental topic. This is partially due to the complexity of segregating multiple variables associated with each pathogen and the challenge of isolating a single mechanism that may be indispensable to the co-infection status. This is further complicated if the pathogens are isolated to different organs. In this study, we employ a unique co-infection model to demonstrate that two important human pathogens occupying anatomically distinct niches have a significant impact on the outcome of both diseases. *S. mansoni* infection during the acute Th1 phase induces misdirection of *H. pylori*-specific T cells to the liver where active helminth-related immune responses take place. *H. pylori* infection and gastritis is associated with the upregulation of pro-inflammatory chemokines like *CXCL9 (MIG)*, *Cxcl 10 (IP-10) Mip-1α*, *Ccl5 (RANTES)*, and *Ccl20* (Eck et al., 2000; Wu et al., 2007; Yamaoka et al., 1998). In addition to these chemokines, our model also showed upregulation of *Ccl4* and *Ccl7* in the stomachs of *H. pylori*-infected animals. Interestingly, during co-infection, we observed that *S. mansoni* (Th1 phase before the development of granulomas) also elicits the production of multiple overlapping pro-inflammatory chemokines in the liver, including *Cxcl 9*, *Cxcl 10*, *Ccl4*, and *Ccl5* among others. Since *H. pylori*-induced T cells express the receptors (CXCR3 and CCR5) for these chemokines and rely on this gradient for arriving at the gastric tissue, the likelihood of their misdirection is high. Indeed, using RNA-seq analysis, we observed that the livers of co-infected mice during the Th1 phase of *S. mansoni* infection express much higher levels of type 1 chemokines like *Cxcl 9* and *Cxcl 10* compared to the stomach. These chemokines are important to recruit the *H. pylori*-specific Th1 cells, and therefore they could be involved in the misdirection of these cells. However, we cannot exclude the possibility that other factors such as shared antigen epitopes between the two pathogens may contribute to misdirection.

Multiple studies have demonstrated the unspecific recruitment of antigen-specific T cells due to an acute infection using transgenic or artificial models (Chen et al., 2005; Ostler et al., 2003; Co et al., 2006). In the current study, *H. pylori*-experienced T cells (during the Th1 phase of schistosome infection) failed to home to the stomach and thus to control *H. pylori* colonization, but rather accumulated within the liver, where the worms mature. This however did not have a noticeable effect on the fecundity or development of adult *S. mansoni* worm pairs nor on egg deposition. The lack of effector function of these T cells on a foreign pathogen is consistent with much of the literature on unspecific trafficking of antigen-specific T cells mentioned above. In this context, it also remains to be determined if this immune misdirection leading to reduced inflammation is specific to concurrent infection with *S. mansoni* or if other acute infections may produce a similar phenotype.

Remarkably, once the peak of the Th2 phase of helminth infection was reached, *H. pylori* colonization was controlled with no further evidence for misdirection of *H. pylori*-specific $CD3^+$ T cells to the liver. At this time, type 1 chemokine levels subsided, and type 2 chemokines were induced. Interestingly, investigation of the liver pathology during this phase revealed an anti-fibrotic effect of *H. pylori*-induced immune responses. Having observed smaller granulomas and lower collagen and ALT levels, we investigated components of the IL-13 pathway that are known to control fibrosis in schistosomiasis and found modulating effects on the induction and recruitment of regulatory T cells as well as on IL-10 and pSTAT3 levels. STAT3 activation in the liver has been demonstrated to be fibrosis protective as it actively prevents hepatocyte damage (Horiguchi et al., 2010; Wang et al., 2010). Hepatocyte specific deletion of STAT3 has also been shown to significantly increase fibrosis (Wang et al., 2011b: Shigekawa et al., 2011). Additionally, activation of STAT3 by IL-10 in macrophages and Kupffer cells is a key anti-inflammatory signal for attenuation of liver inflammation (Horiguchi et al., 2008, 2010; Lafdil et al., 2009; Campana et al., 2018).

During the Th2 phase, *S. mansoni* eggs are known to exploit the Peyer's patches to facilitate their transmission from the host (Turner et al., 2012). Co-incidentally, *H. pylori*-specific T cells are also known to be primed in the Peyer's patches via DCs; this is the primary site for maintenance of the immune response to the bacteria (Nagai et al., 2007; Kiriya et al., 2007). *S. mansoni* eggs as well as *H. pylori* are expert modulators of DCs and could alter their responses, eventually affecting T cell responses and leading to increased IL-10-producing cells.

Interestingly, both pathogens target TLR2-mediated signaling in DCs to induce regulatory phenotypes in these cells (van der Kleij et al., 2002; Sayi et al., 2011; Layland et al., 2007). As we demonstrate *in vitro*, DCs are influenced by the presence of both antigens, cumulatively resulting in increased IL-10 and, upon co-culture, expansion of regulatory T cells. Chronic antigen exposure during these infections may trigger APCs to release more IL-10, an important cytokine to either prime naive $CD4^+$ cells to produce IL-10, suppress inflammatory T cells, and/or increase the differentiation and proliferation of Tregs via STAT3 (Murai et al., 2009; Chaudhry et al., 2011; Hsu et al., 2015; Ye et al., 2007). This may be a complementary effect to the downregulation of type 1 responses by SEA as seen by reduced TNF-α secretion upon co-incubation with the two stimulations (SEA and *H. pylori*). Adding to this, *H. pylori* drives not only Th1/17 responses but also Treg responses, which may contribute to the systemic Treg pool (Lundgren et al., 2003, 2005; Cook et al., 2014).

Another mechanistically important and unexpected finding was the upregulation of IL-13dRa2 transcripts in the livers of

co-infected and *H. pylori*-infected mice during the Th1 phase. This is especially intriguing since *H. pylori* has not been shown to elicit the production of this factor. However, IL-13 has been detected in infected patients, and as the IL-13:IL-13dRa2-interplay consists of a positive feedback loop, the presence of the decoy receptor is plausible (Eskandari-Nasab et al., 2013; Marotti et al., 2008). Interestingly, we could detect significantly higher levels of soluble IL-13dRa2 in the serum of both *H. pylori*-infected individuals as well as in murine samples compared to healthy controls. This is especially important because increased IL-13dRa2 levels can not only impede the process of fibrosis but also significantly reverse its consequences. This decoy receptor has been shown to be protective and prolong host survival during schistosomiasis (Kane et al., 2004). Currently, we believe that the early contribution of the decoy receptor by *H. pylori* systemically acts to induce a protective microenvironment in the liver without strongly affecting antigen-specific responses to *S. mansoni*. In the liver, it scavenges IL-13 induced by immune responses elicited by degrading *S. mansoni* eggs. Subsequently, the increased levels of IL-10 due to co-infection then contribute to control the extent of inflammation and fibrosis. We, however, cannot exclude the possibility that other factors, such as *H.pylori*-induced Tr-1 cells or IFNγ, contribute to the ameliorated liver pathology.

Unfortunately, a reductionist approach to determine the exact mechanism in this co-infection model is extremely challenging. $CD3^+$ cells, IFNγ, and IL-10 are critical to control *H. pylori* infection, while IL-10, IL-13, and IL-13dRa2 are indispensable for the progression as well as protection from fibrosis-related morbidity and mortality in schistosomiasis. Knocking out any of the above factors influences each individual infection alone and would thus not provide us with a clearer picture of the mechanisms regulating the outcome of co-infection. However, treating the animals with the anti-helminthic drug praziquantel may isolate the direct effect of adult schistosome worms on *H. pylori* infection. Still, the effects, if any, induced by the larval stages, juvenile migrating worms, or eggs would remain unaltered as the drug primarily targets adult worms and immunopathology only decreases gradually (Cioli et al., 2014). Using antibiotics to clear *H. pylori* infection on the other hand would alter the microbiome of the gut and thus would not be an ideal approach either, especially since we and others have previously demonstrated a crucial role for the commensal gut bacteria in the egress of schistosoma eggs from the intestinal tissue (Holzscheiter et al., 2014).

Nevertheless, the strength of this model is in the pathological outcome and depicts to a large extent the situation that occurs in people affected by this co-infection. Most individuals have a low-level *H. pylori*-induced inflammation as mimicked by our model, and fewer individuals in these areas show high inflammatory biomarkers associated with gastric neoplasia (Robinson et al., 2007; White et al., 2015; Atherton and Blaser, 2009; Michetti, 2004; Holcombe, 1992). The extent of fibrosis due to chronic schistosomiasis in such co-infected populations has not yet been assessed. A caveat here is that not all schistosome infections in endemic areas follow a clear Th1/Th2 dichotomy, where infection levels differ and reinfection is common. Notwithstanding the above limitations, our study demonstrates a possible mutually beneficial relationship between these chronic pathogens. This is critical as large amounts of funds are currently allocated for the development of prophylactic and therapeutic vaccines against *H. pylori*. This may be extremely beneficial in countries with high gastric cancer risk where *H. pylori*-associated antibiotic resistance is becoming a great concern (Thung et al., 2016; Alba et al., 2017). However, in several countries that experience co-infections, there may be potential side effects. Chronic pathogens have evolved to mutually exist and induce host-protective outcomes in these populations, and elimination of one pathogen without regard to the effects on the other can lead to increased immunopathology of the latter. Additionally, if helminths deviate antigen-specific T cells during acute infection and re-infection or induce bystander immunosuppressive responses during chronic infection, it could lead to inefficient immunization responses post vaccination. The solution could be as simple as treating the patient against the helminth before the vaccination, but without studies that examine these questions, we cannot fully predict the outcome of such strategies.

STAR★METHODS

Detailed methods are provided in the online version of this paper and include the following:

- KEY RESOURCES TABLE
- LEAD CONTACT AND MATERIALS AVAILABILITY
- EXPERIMENTAL MODEL AND SUBJECT DETAILS
  - Mouse
  - Human
- METHOD DETAILS
  - Bacterial strains and culture conditions
  - Experimental *Helicobacter pylori* infection, assessment of colonization and gastric pathology
  - Preparation of gastric single-cell suspensions and flow cytometry
  - Preparation of *H. pylori* lysate
  - Preparation of cells from the lung
  - Schistosoma mansoni infection and evaluation of parasitological parameters
  - In vitro re-stimulation of lymphoid cells
  - Stimulation of liver-associated lymphocytes (LALs) and splenocytes for intracellular cytokine staining and FACS
  - Real-time PCR
  - RNA sequencing
  - Serological and biochemical analysis
  - Adoptive Transfer
  - Immunohistochemistry
  - Co-culture experiments
  - Western blot
- QUANTIFICATION AND STATISTICAL ANALYSIS
- DATA AND CODE AVAILABILITY

SUPPLEMENTAL INFORMATION

Supplemental Information can be found online at https://doi.org/10.1016/j.celrep.2019.05.108.

ACKNOWLEDGMENTS

RNA sequencing was performed at the core facility of Prof. Roland Rad (Klinikum rechts der Isar). Rupert Ollinger performed the library preparation and sequencing. We are grateful to Maximilian Miller (Rutgers University/TU Munich) for input on the manuscript. We would like to thank Marija Ram and Sabine Paul for excellent technical assistance, Matthew Lacorcia for discussions and critical reading of the manuscript, and Professor Michael Vieth (Klinikum Bayreuth) for pathology scoring of the gastric tissue samples. This study was supported by the German Centre for Infection research (DZIF), the Deutsche Forschungsgemeinschaft (DFG)-CO 1469/10-1, and a medical faculty scholarship from the Technical University Munich for S.B.

AUTHOR CONTRIBUTIONS

Conceptualization, S.B., R.M.L., M.G., and C.P.d.C.; Methodology and Investigation, S.B.; Formal Analysis, S.B., E.L.V., A.T., and M.F.; Writing – Original Draft, S.B.; Writing – Review and Editing, R.M.L., E.L.V., M.G., and C.P.d.C.; Funding Acquisition, M.G. and C.P.d.C.; Supervision, M.G. and C.P.d.C.

DECLARATION OF INTEREST

The authors declare no competing interests.

Received: August 2, 2018
Revised: January 29, 2019
Accepted: May 29, 2019
Published: July 2, 2019

REFERENCES

Abou Holw, S.A., Anwar, M.M., Bassiouni, R.B., Hussen, N.A., and Eltaweel, H.A. (2008). Impact of coinfection with Schistosoma mansoni on Helicobacter pylori induced disease. J. Egypt. Soc. Parasitol. *38*, 73–84.

Alba, C., Blanco, A., and Alarcón, T. (2017). Antibiotic resistance in Helicobacter pylori. Curr. Opin. Infect. Dis. *30*, 489–497.

Alemayehu, B., and Tomass, Z. (2015). Schistosoma mansoni infection prevalence and associated risk factors among schoolchildren in Demba Girara, Damot Woide District of Wolaita Zone, Southern Ethiopia. Asian Pac. J. Trop. Med. *8*, 457–463.

Ali, Z., Kosanovic, D., Kolosionek, E., Schermuly, R.T., Graham, B.B., Mathie, A., and Butrous, G. (2017). Enhanced inflammatory cell profiles in schistosomiasis-induced pulmonary vascular remodeling. Pulm. Circ. *7*, 244–252.

Allaker, R.P., Young, K.A., Hardie, J.M., Domizio, P., and Meadows, N.J. (2002). Prevalence of helicobacter pylori at oral and gastrointestinal sites in children: evidence for possible oral-to-oral transmission. J. Med. Microbiol. *51*, 312–317.

Angeli, V., Faveeuw, C., Roye, O., Fontaine, J., Teissier, E., Capron, A., Wolowczuk, I., Capron, M., and Trottein, F. (2001). Role of the parasite-derived prostaglandin D2 in the inhibition of epidermal Langerhans cell migration during schistosomiasis infection. J. Exp. Med. *193*, 1135–1147.

Atherton, J.C., and Blaser, M.J. (2009). Coadaptation of Helicobacter pylori and humans: ancient history, modern implications. J. Clin. Invest. *119*, 2475–2487.

Balakrishnan, M., George, R., Sharma, A., and Graham, D.Y. (2017). Changing Trends in Stomach Cancer Throughout the World. Curr. Gastroenterol. Rep. *19*, 36.

Burke, M.L., Jones, M.K., Gobert, G.N., Li, Y.S., Ellis, M.K., and McManus, D.P. (2009). Immunopathogenesis of human schistosomiasis. Parasite Immunol. *31*, 163–176.

Campana, L., Starkey Lewis, P.J., Pellicoro, A., Aucott, R.L., Man, J., O'Duibhir, E., Mok, S.E., Ferreira-Gonzalez, S., Livingstone, E., Greenhalgh, S.N., et al. (2018). The STAT3-IL-10-IL-6 Pathway Is a Novel Regulator of Macrophage Efferocytosis and Phenotypic Conversion in Sterile Liver Injury. J. Immunol. *200*, 1169–1187.

Cervantes, D.T., Fischbach, L.A., Goodman, K.J., Phillips, C.V., Chen, S., and Broussard, C.S. (2010). Exposure to Helicobacter pylori-positive siblings and persistence of Helicobacter pylori infection in early childhood. J. Pediatr. Gastroenterol. Nutr. *50*, 481–485.

Chaudhry, A., Samstein, R.M., Treuting, P., Liang, Y., Pils, M.C., Heinrich, J.M., Jack, R.S., Wunderlich, F.T., Brüning, J.C., Müller, W., and Rudensky, A.Y. (2011). Interleukin-10 signaling in regulatory T cells is required for suppression of Th17 cell-mediated inflammation. Immunity *34*, 566–578.

Chen, A.M., Khanna, N., Stohlman, S.A., and Bergmann, C.C. (2005). Virus-specific and bystander CD8 T cells recruited during virus-induced encephalomyelitis. J. Virol. *79*, 4700–4708.

Chiaramonte, M.G., Donaldson, D.D., Cheever, A.W., and Wynn, T.A. (1999). An IL-13 inhibitor blocks the development of hepatic fibrosis during a T-helper type 2-dominated inflammatory response. J. Clin. Invest. *104*, 777–785.

Chiaramonte, M.G., Mentink-Kane, M., Jacobson, B.A., Cheever, A.W., Whitters, M.J., Goad, M.E., Wong, A., Collins, M., Donaldson, D.D., Grusby, M.J., and Wynn, T.A. (2003). Regulation and function of the interleukin 13 receptor alpha 2 during a T helper cell type 2-dominant immune response. J. Exp. Med. *197*, 687–701.

Cioli, D., Pica-Mattoccia, L., Basso, A., and Guidi, A. (2014). Schistosomiasis control: praziquantel forever? Mol. Biochem. Parasitol. *195*, 23–29.

Co, D.O., Hogan, L.H., Karman, J., Heninger, E., Vang, S., Wells, K., Kawaoka, Y., and Sandor, M. (2006). Interactions between T cells responding to concurrent mycobacterial and influenza infections. J. Immunol. *177*, 8456–8465.

Cook, K.W., Letley, D.P., Ingram, R.J., Staples, E., Skjoldmose, H., Atherton, J.C., and Robinson, K. (2014). CCL20/CCR6-mediated migration of regulatory T cells to the Helicobacter pylori-infected human gastric mucosa. Gut *63*, 1550–1559.

Dixon, M.F., Genta, R.M., Yardley, J.H., and Correa, P. (1996). Classification and grading of gastritis. The updated Sydney System. International Workshop on the Histopathology of Gastritis, Houston 1994. Am. J. Surg. Pathol. *20*, 1161–1181.

Du, Y., Agnew, A., Ye, X.P., Robinson, P.A., Forman, D., and Crabtree, J.E. (2006). Helicobacter pylori and Schistosoma japonicum co-infection in a Chinese population: helminth infection alters humoral responses to H. pylori and serum pepsinogen I/II ratio. Microbes Infect. *8*, 52–60.

Duncan, M.R., and Berman, B. (1985). Gamma interferon is the lymphokine and beta interferon the monokine responsible for inhibition of fibroblast collagen production and late but not early fibroblast proliferation. J. Exp. Med. *162*, 516–527.

Eck, M., Schmausser, B., Scheller, K., Toksoy, A., Kraus, M., Menzel, T., Müller-Hermelink, H.K., and Gillitzer, R. (2000). CXC chemokines Gro(alpha)/IL-8 and IP-10/MIG in Helicobacter pylori gastritis. Clin. Exp. Immunol. *122*, 192–199.

Erhardt, A., Biburger, M., Papadopoulos, T., and Tiegs, G. (2007). IL-10, regulatory T cells, and Kupffer cells mediate tolerance in concanavalin A-induced liver injury in mice. Hepatology *45*, 475–485.

Eskandari-Nasab, E., Sepanjnia, A., Moghadampour, M., Hadadi-Fishani, M., Rezaeifar, A., Asadi-Saghandi, A., Sadeghi-Kalani, B., Manshadi, M.D., Pourrajab, F., and Pourmasoumi, H. (2013). Circulating levels of interleukin (IL)-12 and IL-13 in Helicobacter pylori-infected patients, and their associations with bacterial CagA and VacA virulence factors. Scand. J. Infect. Dis. *45*, 342–349.

Everts, B., Perona-Wright, G., Smits, H.H., Hokke, C.H., van der Ham, A.J., Fitzsimmons, C.M., Doenhoff, M.J., van der Bosch, J., Mohrs, K., Haas, H., et al. (2009). Omega-1, a glycoprotein secreted by Schistosoma mansoni eggs, drives Th2 responses. J. Exp. Med. *206*, 1673–1680.

Fairfax, K., Nascimento, M., Huang, S.C., Everts, B., and Pearce, E.J. (2012). Th2 responses in schistosomiasis. Semin. Immunopathol. *34*, 863–871.

Fox, J.G., Beck, P., Dangler, C.A., Whary, M.T., Wang, T.C., Shi, H.N., and Nagler-Anderson, C. (2000). Concurrent enteric helminth infection modulates inflammation and gastric immune responses and reduces helicobacter-induced gastric atrophy. Nat. Med. *6*, 536–542.

Franceschi, F., Zuccalà, G., Roccarina, D., and Gasbarrini, A. (2014). Clinical effects of Helicobacter pylori outside the stomach. Nat. Rev. Gastroenterol. Hepatol. *11*, 234–242.

Gatlin, M.R., Black, C.L., Mwinzi, P.N., Secor, W.E., Karanja, D.M., and Colley, D.G. (2009). Association of the gene polymorphisms IFN-gamma +874, IL-13 -1055 and IL-4 -590 with patterns of reinfection with Schistosoma mansoni. PLoS Negl. Trop. Dis. *3*, e375.

Gieseck, R.L., 3rd, Ramalingam, T.R., Hart, K.M., Vannella, K.M., Cantu, D.A., Lu, W.Y., Ferreira-González, S., Forbes, S.J., Vallier, L., and Wynn, T.A. (2016). Interleukin-13 Activates Distinct Cellular Pathways Leading to Ductular Reaction, Steatosis, and Fibrosis. Immunity *45*, 145–158.

Global Atlas of Helminth Infections. (2010). Global burden. http://www.thiswormyworld.org/worms/global-burden.

Guiney, D.G., Hasegawa, P., and Cole, S.P. (2003). Helicobacter pylori preferentially induces interleukin 12 (IL-12) rather than IL-6 or IL-10 in human dendritic cells. Infect. Immun. *71*, 4163–4166.

Haeberlein, S., Obieglo, K., Ozir-Fazalalikhan, A., Chayé, M.A.M., Veninga, H., van der Vlugt, L.E.P.M., Voskamp, A., Boon, L., den Haan, J.M.M., Westerhof, L.B., et al. (2017). Schistosome egg antigens, including the glycoprotein IPSE/alpha-1, trigger the development of regulatory B cells. PLoS Pathog. *13*, e1006539.

Holcombe, C. (1992). Helicobacter pylori: the African enigma. Gut *33*, 429–431.

Holzscheiter, M., Layland, L.E., Loffredo-Verde, E., Mair, K., Vogelmann, R., Langer, R., Wagner, H., and Prazeres da Costa, C. (2014). Lack of host gut microbiota alters immune responses and intestinal granuloma formation during schistosomiasis. Clin. Exp. Immunol. *175*, 246–257.

Hooi, J.K.Y., Lai, W.Y., Ng, W.K., Suen, M.M.Y., Underwood, F.E., Tanyingoh, D., Malfertheiner, P., Graham, D.Y., Wong, V.W.S., Wu, J.C.Y., et al. (2017). Global Prevalence of Helicobacter pylori Infection: Systematic Review and Meta-Analysis. Gastroenterology *153*, 420–429.

Horiguchi, N., Wang, L., Mukhopadhyay, P., Park, O., Jeong, W.I., Lafdil, F., Osei-Hyiaman, D., Moh, A., Fu, X.Y., Pacher, P., et al. (2008). Cell type-dependent pro- and anti-inflammatory role of signal transducer and activator of transcription 3 in alcoholic liver injury. Gastroenterology *134*, 1148–1158.

Horiguchi, N., Lafdil, F., Miller, A.M., Park, O., Wang, H., Rajesh, M., Mukhopadhyay, P., Fu, X.Y., Pacher, P., and Gao, B. (2010). Dissociation between liver inflammation and hepatocellular damage induced by carbon tetrachloride in myeloid cell-specific signal transducer and activator of transcription 3 gene knockout mice. Hepatology *51*, 1724–1734.

Hsu, P., Santner-Nanan, B., Hu, M., Skarratt, K., Lee, C.H., Stormon, M., Wong, M., Fuller, S.J., and Nanan, R. (2015). IL-10 Potentiates Differentiation of Human Induced Regulatory T Cells via STAT3 and Foxo1. J. Immunol. *195*, 3665–3674.

Jankovic, D., Kullberg, M.C., Caspar, P., and Sher, A. (2004). Parasite-induced Th2 polarization is associated with down-regulated dendritic cell responsiveness to Th1 stimuli and a transient delay in T lymphocyte cycling. J. Immunol. *173*, 2419–2427.

Jenh, C.H., Cox, M.A., Cui, L., Reich, E.P., Sullivan, L., Chen, S.C., Kinsley, D., Qian, S., Kim, S.H., Rosenblum, S., et al. (2012). A selective and potent CXCR3 antagonist SCH 546738 attenuates the development of autoimmune diseases and delays graft rejection. BMC Immunol. *13*, 2.

Jimenez, S.A., Freundlich, B., and Rosenbloom, J. (1984). Selective inhibition of human diploid fibroblast collagen synthesis by interferons. J. Clin. Invest. *74*, 1112–1116.

Käbisch, R., Semper, R.P., Wüstner, S., Gerhard, M., and Mejías-Luque, R. (2016). Helicobacter pylori γ-Glutamyltranspeptidase Induces Tolerogenic Human Dendritic Cells by Activation of Glutamate Receptors. J. Immunol. *196*, 4246–4252.

Kaebisch, R., Mejías-Luque, R., Prinz, C., and Gerhard, M. (2014). Helicobacter pylori cytotoxin-associated gene A impairs human dendritic cell maturation and function through IL-10-mediated activation of STAT3. J. Immunol. *192*, 316–323.

Kane, C.M., Cervi, L., Sun, J., McKee, A.S., Masek, K.S., Shapira, S., Hunter, C.A., and Pearce, E.J. (2004). Helminth antigens modulate TLR-initiated dendritic cell activation. J. Immunol. *173*, 7454–7461.

Kiriya, K., Watanabe, N., Nishio, A., Okazaki, K., Kido, M., Saga, K., Tanaka, J., Akamatsu, T., Ohashi, S., Asada, M., et al. (2007). Essential role of Peyer's patches in the development of Helicobacter-induced gastritis. Int. Immunol. *19*, 435–446.

Knolle, P.A., Uhrig, A., Protzer, U., Trippler, M., Duchmann, R., Meyer zum Büschenfelde, K.H., and Gerken, G. (1998). Interleukin-10 expression is autoregulated at the transcriptional level in human and murine Kupffer cells. Hepatology *27*, 93–99.

Lafdil, F., Wang, H., Park, O., Zhang, W., Moritoki, Y., Yin, S., Fu, X.Y., Gershwin, M.E., Lian, Z.X., and Gao, B. (2009). Myeloid STAT3 inhibits T cell-mediated hepatitis by regulating T helper 1 cytokine and interleukin-17 production. Gastroenterology *137*, 2125–2135.e1-2.

Layland, L.E., Rad, R., Wagner, H., and da Costa, C.U. (2007). Immunopathology in schistosomiasis is controlled by antigen-specific regulatory T cells primed in the presence of TLR2. Eur. J. Immunol. *37*, 2174–2184.

Layland, L.E., Mages, J., Loddenkemper, C., Hoerauf, A., Wagner, H., Lang, R., and da Costa, C.U. (2010). Pronounced phenotype in activated regulatory T cells during a chronic helminth infection. J. Immunol. *184*, 713–724.

Love, M.I., Huber, W., and Anders, S. (2014). Moderated estimation of fold change and dispersion for RNA-seq data with DESeq2. Genome Biol. *15*, 550.

Lundgren, A., Suri-Payer, E., Enarsson, K., Svennerholm, A.M., and Lundin, B.S. (2003). Helicobacter pylori-specific CD4+ CD25high regulatory T cells suppress memory T-cell responses to H. pylori in infected individuals. Infect. Immun. *71*, 1755–1762.

Lundgren, A., Strömberg, E., Sjöling, A., Lindholm, C., Enarsson, K., Edebo, A., Johnsson, E., Suri-Payer, E., Larsson, P., Rudin, A., et al. (2005). Mucosal FOXP3-expressing CD4+ CD25high regulatory T cells in Helicobacter pylori-infected patients. Infect. Immun. *73*, 523–531.

Macosko, E.Z., Basu, A., Satija, R., Nemesh, J., Shekhar, K., Goldman, M., Tirosh, I., Bialas, A.R., Kamitaki, N., Martersteck, E.M., et al. (2015). Highly Parallel Genome-wide Expression Profiling of Individual Cells Using Nanoliter Droplets. Cell *161*, 1202–1214.

Marotti, B., Rocco, A., De Colibus, P., Compare, D., de Nucci, G., Staibano, S., Tatangelo, F., Romano, M., and Nardone, G. (2008). Interleukin-13 mucosal production in Helicobacter pylori-related gastric diseases. Dig. Liver Dis. *40*, 240–247.

Mathurin, P., Xiong, S., Kharbanda, K.K., Veal, N., Miyahara, T., Motomura, K., Rippe, R.A., Bachem, M.G., and Tsukamoto, H. (2002). IL-10 receptor and coreceptor expression in quiescent and activated hepatic stellate cells. Am. J. Physiol. Gastrointest. Liver Physiol. *282*, G981–G990.

McKee, A.S., and Pearce, E.J. (2004). CD25+CD4+ cells contribute to Th2 polarization during helminth infection by suppressing Th1 response development. J. Immunol. *173*, 1224–1231.

Mentink-Kane, M.M., Cheever, A.W., Thompson, R.W., Hari, D.M., Kabatereine, N.B., Vennervald, B.J., Ouma, J.H., Mwatha, J.K., Jones, F.M., Donaldson, D.D., et al. (2004). IL-13 receptor alpha 2 down-modulates granulomatous inflammation and prolongs host survival in schistosomiasis. Proc. Natl. Acad. Sci. USA *101*, 586–590.

Michetti, P. (2004). Experimental Helicobacter pylori infection in humans: a multifaceted challenge. Gut *53*, 1220–1221.

Miyaji, H., Azuma, T., Ito, S., Abe, Y., Gejyo, F., Hashimoto, N., Sugimoto, H., Suto, H., Ito, Y., Yamazaki, Y., et al. (2000). Helicobacter pylori infection occurs via close contact with infected individuals in early childhood. J. Gastroenterol. Hepatol. *15*, 257–262.

Murai, M., Turovskaya, O., Kim, G., Madan, R., Karp, C.L., Cheroutre, H., and Kronenberg, M. (2009). Interleukin 10 acts on regulatory T cells to maintain expression of the transcription factor Foxp3 and suppressive function in mice with colitis. Nat. Immunol. *10*, 1178–1184.

Nagai, S., Mimuro, H., Yamada, T., Baba, Y., Moro, K., Nochi, T., Kiyono, H., Suzuki, T., Sasakawa, C., and Koyasu, S. (2007). Role of Peyer's patches in

the induction of Helicobacter pylori-induced gastritis. Proc. Natl. Acad. Sci. USA *104*, 8971–8976.

Ogawa, H., Iwamoto, A., Tanahashi, T., Okada, R., Yamamoto, K., Nishiumi, S., Yoshida, M., and Azuma, T. (2017). Genetic variants of *Helicobacter pylori* type IV secretion system components CagL and CagI and their association with clinical outcomes. Gut Pathog. *9*, 21.

Ostler, T., Pircher, H., and Ehl, S. (2003). "Bystander" recruitment of systemic memory T cells delays the immune response to respiratory virus infection. Eur. J. Immunol. *33*, 1839–1848.

Parekh, S., Ziegenhain, C., Vieth, B., Enard, W., and Hellmann, I. (2016). The impact of amplification on differential expression analyses by RNA-seq. Sci. Rep. *6*, 25533.

Rabelo-Gonçalves, E.M., Roesler, B.M., and Zeitune, J.M. (2015). Extragastric manifestations of Helicobacter pylori infection: Possible role of bacterium in liver and pancreas diseases. World J. Hepatol. *7*, 2968–2979.

Robinson, K., Argent, R.H., and Atherton, J.C. (2007). The inflammatory and immune response to Helicobacter pylori infection. Best Pract. Res. Clin. Gastroenterol. *21*, 237–259.

Rocha, M., Avenaud, P., Ménard, A., Le Bail, B., Balabaud, C., Bioulac-Sage, P., de Magalhães Queiroz, D.M., and Mégraud, F. (2005). Association of Helicobacter species with hepatitis C cirrhosis with or without hepatocellular carcinoma. Gut *54*, 396–401.

Rothenbacher, D., Inceoglu, J., Bode, G., and Brenner, H. (2000). Acquisition of Helicobacter pylori infection in a high-risk population occurs within the first 2 years of life. J. Pediatr. *136*, 744–748.

Sadler, C.H., Rutitzky, L.I., Stadecker, M.J., and Wilson, R.A. (2003). IL-10 is crucial for the transition from acute to chronic disease state during infection of mice with Schistosoma mansoni. Eur. J. Immunol. *33*, 880–888.

Sayi, A., Kohler, E., Toller, I.M., Flavell, R.A., Müller, W., Roers, A., and Müller, A. (2011). TLR-2-activated B cells suppress Helicobacter-induced preneoplastic gastric immunopathology by inducing T regulatory-1 cells. J. Immunol. *186*, 878–890.

Shigekawa, M., Takehara, T., Kodama, T., Hikita, H., Shimizu, S., Li, W., Miyagi, T., Hosui, A., Tatsumi, T., Ishida, H., et al. (2011). Involvement of STAT3-regulated hepatic soluble factors in attenuation of stellate cell activity and liver fibrogenesis in mice. Biochem. Biophys. Res. Commun. *406*, 614–620.

Shimizu, T., Chiba, T., and Marusawa, H. (2017). Helicobacter pylori-Mediated Genetic Instability and Gastric Carcinogenesis. Curr. Top. Microbiol. Immunol. *400*, 305–323.

Spencer, S.A., Penney, J.M.S.J., Russell, H.J., Howe, A.P., Linder, C., Rakotomampianina, A.L.D., Nandimbiniaina, A.M., Squire, S.B., Stothard, J.R., Bustinduy, A.L., and Rahetilahy, A.M. (2017). High burden of Schistosoma mansoni infection in school-aged children in Marolambo District, Madagascar. Parasit. Vectors *10*, 307.

Stross, L., Günther, J., Gasteiger, G., Asen, T., Graf, S., Aichler, M., Esposito, I., Busch, D.H., Knolle, P., Sparwasser, T., and Protzer, U. (2012). Foxp3+ regulatory T cells protect the liver from immune damage and compromise virus control during acute experimental hepatitis B virus infection in mice. Hepatology *56*, 873–883.

Teixeira-Carvalho, A., Martins-Filho, O.A., Peruhype-Magalhães, V., Silveira-Lemos, D., Malaquias, L.C., Oliveira, L.F., Silveira, A.M., Gazzinelli, A., Gazzinelli, G., and Corrêa-Oliveira, R. (2008). Cytokines, chemokine receptors, CD4+CD25HIGH+ T-cells and clinical forms of human schistosomiasis. Acta Trop. *108*, 139–149.

Thung, I., Aramin, H., Vavinskaya, V., Gupta, S., Park, J.Y., Crowe, S.E., and Valasek, M.A. (2016). Review article: the global emergence of Helicobacter pylori antibiotic resistance. Aliment. Pharmacol. Ther. *43*, 514–533.

Turner, J.D., Narang, P., Coles, M.C., and Mountford, A.P. (2012). Blood flukes exploit Peyer's Patch lymphoid tissue to facilitate transmission from the mammalian host. PLoS Pathog. *8*, e1003063.

van der Kleij, D., Latz, E., Brouwers, J.F., Kruize, Y.C., Schmitz, M., Kurt-Jones, E.A., Espevik, T., de Jong, E.C., Kapsenberg, M.L., Golenbock, D.T., et al. (2002). A novel host-parasite lipid cross-talk. Schistosomal lyso-phosphatidylserine activates toll-like receptor 2 and affects immune polarization. J. Biol. Chem. *277*, 48122–48129.

Wang, H., Park, O., Lafdil, F., Shen, K., Horiguchi, N., Yin, S., Fu, X.Y., Kunos, G., and Gao, B. (2010). Interplay of hepatic and myeloid signal transducer and activator of transcription 3 in facilitating liver regeneration via tempering innate immunity. Hepatology *51*, 1354–1362.

Wang, H., Lafdil, F., Kong, X., and Gao, B. (2011a). Signal transducer and activator of transcription 3 in liver diseases: a novel therapeutic target. Int. J. Biol. Sci. *7*, 536–550.

Wang, H., Lafdil, F., Wang, L., Park, O., Yin, S., Niu, J., Miller, A.M., Sun, Z., and Gao, B. (2011b). Hepatoprotective versus oncogenic functions of STAT3 in liver tumorigenesis. Am. J. Pathol. *179*, 714–724.

White, J.R., Winter, J.A., and Robinson, K. (2015). Differential inflammatory response to Helicobacter pylori infection: etiology and clinical outcomes. J. Inflamm. Res. *8*, 137–147.

World Health Organization (2017). Cancer fact sheet. http://www.who.int/mediacentre/factsheets/fs297/en/.

World Health Organization (2019). Schistosomiasis fact sheet. http://www.who.int/mediacentre/factsheets/fs115/en/.

Wu, Y.Y., Tsai, H.F., Lin, W.C., Hsu, P.I., Shun, C.T., Wu, M.S., and Hsu, P.N. (2007). Upregulation of CCL20 and recruitment of CCR6+ gastric infiltrating lymphocytes in Helicobacter pylori gastritis. Infect. Immun. *75*, 4357–4363.

Wynn, T.A. (2003). IL-13 effector functions. Annu. Rev. Immunol. *21*, 425–456.

Xuan, S.Y., Li, N., Qiang, X., Zhou, R.R., Shi, Y.X., and Jiang, W.J. (2006). Helicobacter infection in hepatocellular carcinoma tissue. World J. Gastroenterol. *12*, 2335–2340.

Yamaoka, Y., Kita, M., Kodama, T., Sawai, N., Tanahashi, T., Kashima, K., and Imanishi, J. (1998). Chemokines in the gastric mucosa in Helicobacter pylori infection. Gut *42*, 609–617.

Ye, Z., Huang, H., Hao, S., Xu, S., Yu, H., Van Den Hurk, S., and Xiang, J. (2007). IL-10 has a distinct immunoregulatory effect on naive and active T cell subsets. J. Interferon Cytokine Res. *27*, 1031–1038.

Yue, C., Shen, S., Deng, J., Priceman, S.J., Li, W., Huang, A., and Yu, H. (2015). STAT3 in CD8+ T Cells Inhibits Their Tumor Accumulation by Downregulating CXCR3/CXCL10 Axis. Cancer Immunol. Res. *3*, 864–870.

Zhang, X., Han, J., Man, K., Li, X., Du, J., Chu, E.S., Go, M.Y., Sung, J.J., and Yu, J. (2016). CXC chemokine receptor 3 promotes steatohepatitis in mice through mediating inflammatory cytokines, macrophages and autophagy. J. Hepatol. *64*, 160–170.

STAR★METHODS

KEY RESOURCES TABLE

REAGENT or RESOURCE	SOURCE	IDENTIFIER
Antibodies		
CD3 Monoclonal Antibody (17A2)	Thermo Fisher	Cat# 14-0032-82, RRID:AB_467053
CD28 Monoclonal Antibody (37.51)	Thermo Fisher	Cat# 16-0281-82, RRID:AB_468921
APC anti-mouse CD4 Antibody (RM4-5)	Biolegend	Cat# 100516, RRID:AB_312719
PE/Cy7 anti-mouse CD4 Antibody	Biolegend	Cat# 100528, RRID:AB_312729
CD8a Rat anti-Mouse, APC-H7, Clone: 53-6.7	BD	Cat# 560247, RRID:AB_1645238
IL-10 Monoclonal Antibody (JES5-16E3), FITC	Thermo Fisher	Cat# 11-7101-41, RRID:AB_2572513
FOXP3 Monoclonal Antibody (FJK-16 s), eFluor 450	Thermo Fisher	Cat# 48-5773-82, RRID:AB_1518812
IFN gamma Monoclonal Antibody (XMG1.2)	Thermo Fisher	Cat# 16-7311-81, RRID:AB_469242
APC anti-mouse CD45.1 Antibody	Biolegend	Cat# 110714, RRID:AB_313503
FITC anti-mouse CD45.2 Antibody	Biolegend	Cat# 109806, RRID:AB_313443
APC anti-mouse CD183 (CXCR3) Antibody	Biolegend	Cat# 126512, RRID:AB_1088993
CCR5 Monoclonal Antibody (HEK/1/85a), FITC	Thermo Fisher	Cat# MA1-20282, RRID:AB_558101
PE anti-mouse/human CD44 Antibody (IM7)	Biolegend	Cat# 103024, RRID:AB_493687
PE/Cy7 anti-mouse/human CD44 Antibody	Biolegend	Cat# 103030, RRID:AB_830787
Anti-IL-10 antibody	Abcam	Cat# ab189392, RRID:AB_298637
Phospho-Stat3	Cell Signaling	Cat#9145S, RRID:AB_2491009
Stat3	Cell Signaling	Cat# 9139S, RRID:AB_331757
GAPDH	Cell Signaling	Cat# 2118S, RRID:AB_561053
Bacterial and Virus Strains		
Helicobacter pylori PMSS1	Gift from Anne Mueller	https://www.imcr.uzh.ch/en/research/Muller/Team/Muller.html
Chemicals, Peptides, and Recombinant Proteins		
Percoll	Millipore Sigma	P1644-100ML, CAS:65455-52-9
Brefeldin A	Millipore Sigma	B5936-200UL, CAS:20350-15-6
PMA	Millipore Sigma	P1585-1MG, CAS:16561-29-8
Ionomycin	Millipore Sigma	407953-2MG, CAS:56092-82-1
SCH 546738	MCE	HY-10017, CAS:906805-42-3
Critical Commercial Assays		
Pan T Cell Isolation Kit II, mouse	Milteny Biotec	130-095-130
Total Collagen Assay	Quickzyme	QZBtotcol2
Total Protein Assay	Quickzyme	QZBtotprot2
Invitrogen ebioscience Mouse IFN gamma ELISA Ready-SET-Go	Fischer scientific	50-112-9023
Mouse IL-10 DuoSet ELISA	R&D Systems	DY417
Mouse IL-13 R alpha 2 Quantikine ELISA Kit	R&D Systems	M13RA2
IL-13RA2 Human ELISA Kit	Thermo Fisher	EHIL13RA2
Deposited Data		
European Nucleotide Archive (ENA)	This paper	Accession# ENA: PRJEB32256 Study name: ena-STUDY-Technical university munich, Instiitute for medical microbiology, immunology and hygiene-21-04-2019-00:13:28:705-172
Experimental Models: Organisms/Strains		
C57BL/6 mice	Envigo	C57BL6/JOlaHsd

(*Continued on next page*)

Continued

REAGENT or RESOURCE	SOURCE	IDENTIFIER
Oligonucleotides		
Ifng- TCAAGTGGCATAGATGTGGAAGAA TGGCTCTGCAGGATTTTCARG	Millipore Sigma	N/A
Tnfa- CGATGGGTTGTACCTTGTC CGGACTCCGCAAAGTCTAAG	Millipore Sigma	N/A
Mip-2- AGTGAACTGCGCTGTCAATGC AGGCAAACTTTTTGACCGCC	Millipore Sigma	N/A
Foxp3- AGGAGCCGCAAGCTAAAAGC TGCCTTCGTGCCCACTGT	Millipore Sigma	N/A
Ccl5- CAC CAC TCC CTG CTG CTT ACA CTT GGC GGT TCC TTC	Millipore Sigma	N/A
Gapdh- GCCTTCTCCATGGTGGTGAA GCACAGTCAAGGCCGAGAAT	Millipore Sigma	N/A
Hprt- GCCGAGGATTTGGAAAAAGT TATAGCCCCCCTTGAGCACA	Millipore Sigma	N/A
Software and Algorithms		
PRISM® 7	Graph- Pad Software Inc., San Diego, CA, USA	N/A
FlowJo 10 software	Tree Star	N/A
DESeq2 package (version 1.16.1)	N/A	N/A

LEAD CONTACT AND MATERIALS AVAILABILITY

Further information and requests for resources and reagents should be directed to and will be fulfilled by: Prof. Dr. med. Clarissa Prazeres da Costa (clarissa.dacosta@tum.de).

EXPERIMENTAL MODEL AND SUBJECT DETAILS

Mouse

Female C57BL/6 mice, 6–8 weeks old, were purchased from Envigo (Germany) and maintained under specific pathogen-free (spf) conditions at the Institute of Medical Microbiology, Immunology and Hygiene (MIH), TU Munich. All experiments were performed in accordance with and approved by local government authorities of Regierung von Oberbayern (AZ. 55.2.1.54-2532-85-2016). For the Th1/acute phase experiments, we first infected C57BL/6 mice with *H. pylori* (PMSS1). 5.5 weeks later, when *H. pylori* infection reaches chronicity, these mice were subcutaneously infected with *S. mansoni*. After 5.5 weeks of schistosome infection (corresponding to the peak of the Th1 phase, we investigated *H. pylori* colonization and gastric inflammation as well as *S. mansoni* associated parameters. For the Th2/chronic phase mice were infected with *H. pylori* for 5.5 weeks before the infection with schistosomes, then sacrificed during the peak of the Th2 phase after 9.5 weeks of *S. mansoni* infection.

Human

Serum samples obtained from adult *H. pylori* infected individuals and controls were approved by the local ethical committee of the Technical University Munich (5662-13S-2016). The samples obtained were from mixed genders for both groups and did not display any gender bias with regard to immune responses or *H. pylori* antigen status.

METHOD DETAILS

Bacterial strains and culture conditions

H. pylori strain PMSS1 (*H. pylori* pre mouse Sydney strain 1) was used in all experiments, both in-vitro and in-vivo. Bacteria were plated on Wilkins Chalgren (WC) blood agar plates supplemented with Dent (Oxiod) and cultured in a microaerophilic (5% O_2, 10% CO_2) humidified incubator at 37 degrees; split every two days. Bacteria were stored in aliquots in freezing media containing BB-Dent, 20%FCS and 20% glycerol at −80°C and freshly thawed and cultured for each infection to obtain motile and viable *H. pylori*.

Experimental *Helicobacter pylori* infection, assessment of colonization and gastric pathology

6- to 8-wk-old female C57BL/6 were orally gavaged with three doses of *H. pylori* strain PMSS1 ($2x10^8$ CFUs) on alternate days within a week. After mice were sacrificed, the stomach was dissected along the lesser curvature, washed with PBS, and sectioned

longitudinally into equal strips. Sectional similarity was maintained for each mouse assigned to downstream processing in order to minimize sampling error. H. pylori colonization was assessed by plating serial dilutions of stomach extracts. Tissue pathology was assessed by an independent pathologist according to the updated Sydney score system (Dixon et al., 1996).

Preparation of gastric single-cell suspensions and flow cytometry

For the isolation of gastric immune cells, a stomach section was weighed and digested in 1 mg/ml collagenase (Sigma-Aldrich) ± 200 μg/ml Dnase I (Roche) for 30 min at 37°C with shaking. Single-cell suspensions were filtered and stained for CD3, CD4CD45, CXCR3, CCR5 and CD44 (Thermo Fisher). Flow cytometry was performed on a Cytoflex (Beckman Coulter) and analyzed using FlowJo 10 software (Tree Star).

Preparation of *H. pylori* lysate

H. pylori PMSS1 was cultured for 2 days on WC Dent plates. Bacteria was then collected in PBS, washed after centrifugation and re-suspended in fresh PBS. This was followed by sonication on ice (20x with 1 minute breaks). BCA assay (Bio-Rad) was performed to determine protein concentration.

Preparation of cells from the lung

Briefly, the lungs were cut into small pieces and placed into a collagenase (Sigma-Aldrich)/ DNase (Roche) digest solution and incubated at 37°C under constant shaking for 45min. The digested lungs were passed through a 100μm cell strainer. The filtrate was centrifuged and the resulting supernatant was discarded. The pellet was washed twice and erythrocyte lysis (ACK buffer) was performed. Finally, cells were washed again with 20 PBS/2% FCS, centrifuged, the pellet re-suspended and counted for flow cytometry assays. Flow cytometry was performed on a Cytoflex (Beckman Coulter) and analyzed using FlowJo 10 software (Tree Star).

Schistosoma mansoni infection and evaluation of parasitological parameters

Female C57BL/6 mice (6 to 8 weeks) were infected with *S. mansoni* subcutaneously as previously described (Layland et al., 2007). *S. mansoni* infection was confirmed through stool PCR as well as by enumeration of parasite egg burden following digestion of liver samples in potassium hydroxide solution (Merck) as described before. Paraffin embedded sections (3 μm) from the median liver lobe of each mouse were stained with Masson's blue to microscopically determine granuloma sizes as described previously (Layland et al., 2007). Collagen levels were quantified relative to protein levels from paraffin embedded sections using the QuickZyme® Total Collagen assay and QuickZyme protein assay (QuickZyme Biosciences, the Netherlands) respectively, according to manufacturer's instructions.

In vitro re-stimulation of lymphoid cells

Erythrocyte-depleted cell suspensions ($3x10^5$cells) from individual mesenteric lymph nodes (MLN) and spleens were re-stimulated *in vitro* for 48 hours with αCD3 and αCD28 coated MicroBeads (Miltenyi Biotec) in a cell to bead ratio of 1:1. For *S. mansoni* specific re-stimulation, cells were stimulated with 20 μg/ml soluble egg antigen (SEA) prepared from *S. mansoni* eggs. Cytokine content in the culture supernatant was determined using Ready-Set-Go® ELISAs (Thermo Fisher) and Duo Set® ELISAs (R&D Systems) in accordance with the manufacturer's instructions.

Stimulation of liver-associated lymphocytes (LALs) and splenocytes for intracellular cytokine staining and FACS

LALs were prepared from mouse livers, isolated with a percoll gradient as described previously (Stross et al., 2012). Erythrocyte-depleted cell suspensions ($1x10^6$) were re-stimulated with PMA (50 ng/ml) and Ionomycin (1μg/ml) for 1.5 hours followed by 13,5 μg/ml brefeldin A (Sigma-Aldrich) for 3.5 hours.

For flow cytometric analyses, LALs and splenocytes were stained with ethidium monoazide bromide, anti-CD4, anti-CD8, anti-Foxp3, anti-IL-10, anti-IFN-γ and anti-CD4 PE-TexasRed (Invitrogen). For intracellular staining, cells were permeabilized and fixed after surface staining using the Foxp3 staining buffer set (eBioscience) or Cytofix kit (BD) according to manufacturer's instructions. Flow cytometric analysis was perfomed on a Cytoflex machine (Beckman Coulter) and data was analyzed using FlowJo version 10 (Tree Star).

Real-time PCR

Cytokine and chemokine mRNA expression was determined by RT-PCR. Total tissue RNA was isolated using RNA isolation kit (QIAGEN). RNA (1 μg) was retrotranscribed (M-MLV (-) reverse transcriptase, Promega). Primers were designed using the Roche Universal Probe Library system in conjunction with the appropriate probes and the samples were then used for real-time PCR (CFX Bio-Rad). Absolute values were normalized to *Gapdh* expression for stomach and *Hprt* for liver and further to Naive mice using the ddCT method.

RNA sequencing

RNA was isolated from stomach and liver samples as indicated in the previous section and all samples were diluted at 5μg/μl. The Library for bulk 3′-sequencing of poly(A)-RNA was prepared as described previously (Parekh et al., 2016). Briefly, barcoded cDNA of

each sample was generated with a Maxima RT polymerase (Thermo Fisher) using oligo-dT primer containing barcodes, unique molecular identifiers (UMIs) and an adaptor. 5′ ends of the cDNAs were extended by a template switch oligo (TSO) and full-length cDNA was amplified with primers binding to the TSO-site and the adaptor. cDNA was tagmented with the Nextera XT kit (Illumina) and 3′ end-fragments finally amplified using primers with Illumina P5 and P7 overhangs. The library was sequenced on a NextSeq 500 (Illumina) with 75 cycles for the cDNA in read1 and 16 cycles for the barcodes and UMIs in read2. Data were processed as described in Macosko et al. (2015). In brief, the reads were demultiplexed for the sample barcode and mapped. Then these reads were filtered for unique molecular identifiers. The numbers in the DGE Matrix therefore represented counts of reads that map to the specified gene and have a unique identifier. For the identification of differentially expressed genes we used the DESeq2 package (version 1.16.1) employing a one-factor design with four levels (mono-infected stomach, co-infected stomach, mono-infected liver and co-infected liver) (Love et al., 2014). Genes with a minimum fold change of two and an adjusted p value smaller than 0.1 were considered differentially expressed. Principal component analysis was done following DESeq2 variance stabilizing transformation using the R function "prcomp."

Serological and biochemical analysis

Alanine aminotransferase (ALT) levels from serum were measured on the Reflotron Clinical Chemistry analyzer (Roche). Murine serum IL-13 Rα2 levels were detected using the IL-13 Rα2 Quantikine ELISA kit (R&D Systems) according to the manufacturer's instructions. Human IL-13dRa2 levels in the serum were detected using the Human IL-13Ra2 ELISA kit (Invitrogen) according to manufacturer's instructions.

Adoptive Transfer

For adoptive transfer experiments, $CD44^{hi}$ $CD4^{+}$ and $CD8^{+}$ T cells were isolated using the MACS Pan T cell isolation kit (Miltenyi Biotec) followed by cell sorting (MoFlo) from MLN, stomach and peyer's patches of *H.pylori* infected CD45.1 congenic mice. 10^5 of these cells were then transferred intravenously to the respective recipient mice. Mice were sacrificed 3 days later and the stomach, liver, lungs, spleen, MLN and blood were processed as described before. Cells were stained for CD45.1 APC, CD45.2 FITC, CD4 eFluor450, CD8 APC H7 (BD), CD44 PECy-7 and CXCR3 PE. All antibodies were provided by eBioscience / Thermo Fisher unless otherwise stated.

For blocking CXCR3 on T cells, SCH546738 was used in-vitro as described before (Jenh et al., 2012; Zhang et al., 2016; Yue et al., 2015). CD45.1, $CD44^{hi}$ T cells were sorted and exposed to 100nM of the compound (RPMI /0.01%DMSO) for 3 hours at 37 degrees/ 5%CO_2, following blocking, cells were washed, re-suspended in PBS and 10^5 cells were intravenously transferred into each of the CD45.2 experimental groups. Before transfer, cell viability was analyzed using the ViCell cell counter (Beckman Coulter).

Immunohistochemistry

Paraffin embedded tissue pieces were cut in 2μm sections and processed as described before. Briefly, sections were deparaffinised at 60 degrees, followed by sequential dehydration and then boiled in 0.01M Sodium citrate solution (pH 6). Sections were treated with 3% H_2O_2 to inhibit endogenous peroxidase and then blocked with 5% Goat serum. For IL10 detection, 10% H_2O_2 was used. Primary antibodies against CD3 (Thermo Fischer) or IL10 (Abcam) were applied at 4 degrees overnight according to manufacturer's instructions, followed by multiple washing steps and application of the corresponding HRP labeled secondary antibody (Promega). For detection, a DAB (Cell signaling) solution was applied followed by hematoxylin counter stain and subsequent dehydration steps before the slides were mounted with Roti-Mount (Carl-Roth). Imaging was done using the Olympus Slide scanner.

Co-culture experiments

For generation of murine bone marrow–derived dendritic cells (BMDCs), bone marrow was obtained from the tibia and femur of Naive donor mice. Cells were cultured for 7 d at 37°C in RPMI 1640 medium containing 10% FCS (Sigma-Aldrich), 1% penicillin/streptomycin (Life Technologies), 50 μM 2-ME (Sigma-Aldrich), and 20 ng/ml GM-CSF (Miltenyi Biotec). BMDCs were stimulated with SEA (20μg/ml), *H. pylori* PMSS1 (MOI 5) or both simultaneously. LPS (10ng) and SEA+LPS were used as a control. Following overnight stimulation, BMDCs were treated with Gentamycin (100μg/ml) for 0.5h in order to kill *H. pylori*, prior to the addition of T cells.

T cells were isolated using the $CD4^{+}$ or $CD4^{+}$ $CD62L^{+}$ cell isolation kit (Miltenyi Biotec), according to manufacturer's instructions. Cells were loaded in double the proportion to dendritic cells (2:1). Supernatant was collected on day 3 and 7, cells were harvested after 7d for FACS analysis.

Western blot

Tissue samples were prepared using RIPA buffer with protease and phosphatase inhibitors. 10μl of lysate were loaded per well. After transferring, membranes were blocked in TBS-T containing 5% skim milk. pSTAT3 or IL10 antibody (Abcam) was applied following manufacturer instructions o/n. After washing, membranes were incubated for 1 hour at RT with anti-rat HRP conjugated secondary antibody (Promega) diluted 1/2000 in TBS-T-5%BSA. Samples were developed using BioRad developing solution. Images were acquired on an Intas developing system.

QUANTIFICATION AND STATISTICAL ANALYSIS

Sample size for each group in all experiments was pre-determined by a statistician based on parameters associated with both pathogens and the standard deviation of the quantitative data from previous experiments. All other statistical analysis was performed using PRISM® 7 (Graph- Pad Software Inc., San Diego, CA, USA). D'Agostino and Pearson omnibus normality tests were performed to assess the nature of the datasets, parametrically distributed data were analyzed using the unpaired t test (2 groups) and Mann-Whitney U-test was used for nonparametric data. For more than two groups, 1-way ANOVA was conducted, if significant, a multiple comparison analysis was performed. For nonparametric data, a Kruskal–Wallis test with a confidence interval of 95% was employed. Results with a *P value* of < 0.05 were considered as significant. Stars indicate significance, n indicates number of mice and the description for both is indicated in each figure legend.

Any animals grouped as 'co-infected' that later did not have CFU (*H. pylori* infection) or eggs as determined through parasitological screening (*S. mansoni* infection-Th2 phase) were excluded from the analysis.

DATA AND CODE AVAILABILITY

Raw and Meta data associated with RNA sequencing is available on the European Nucleotide Archive (ENA) under Accession # ENA: PRJEB32256. The study name is ena-STUDY-Technical university munich, Instiitute for medical microbiology, immunology and hygiene-21-04-2019-00:13:28:705-172.